Analysis of interaction between *Bacillus thuringiensis* Cry1A Toxins and Epithelial Cell Membrane of Insect Midguts

Name: Kazuya Tomimoto

Doctoral Program in Life and Food Science

Graduate School of Science and Technology

Niigata University

TABLE OF CONTENTS

General introduction

Bacillus thuringiensis is Gram-positive soil bacteria which produces insecticidal crystal protein (ICP). Recent reports suggests that the ICP is synthesized in an inclusion body and the toxic protein comprising ICP is named δ-endotoxin. δ-endotoxin is highly and specifically toxic against various families in mainly Lepidoptera embracing butterfly, moth, etc., and Diptera belonging fly, mosquito and so on. The essence of *B. thuringiensis* δ-endotoxin is a protein called Cry toxin; the toxin was named Cry after the “crystal”. Historically, Cry toxin was categorized into four classes from the specificity of insecticidal activity (Höfte and Whiteley, 1989). Class I (CryI) is specific to lepidoptera, Class II (CryII) is toxic to lepidoptera and diptera, Class III (CryIII) kills coleoptera such as beetle, goldbug, etc., and Class IV (CryIV) displays an insecticidal activity toward diptera. This grouping has been useful because researcher can easily and instructively understand the relationship between a Cry toxin and its insecticidality; however, this classification connotes some inconveniences as well as advantages. The classification requires bioassay to determine the insecticidal activity when registering new Cry toxin, and furthermore, the categorization does not consider about the genetic homology and similarity among Cry toxins. Therefore, Crickmore and his coworker advocated new categorization of Cry toxins based on only the nucleotide sequence to solve these disadvantages (Crickmore et al., 1998), so far, this grouping has been used in consensus.

Cry1 toxins comprising Cry1Aa, Cry1Ab, Cry1Ac etc., is the lepidopteran insect specific toxin and is the mainly investigated Cry toxin. After susceptible lepidopteran larvae ingests Cry1A toxin, the crystal is solubilized to 130 kDa protoxin by alkaline midgut juice. Thereafter, the protoxin is truncated at C-terminal half by trypsin-like protease in midgut fluid and activated to 65 kDa Cry toxin is resulted (Ogiwara et al., 1992; Milne and Kaplan, 1993; Oppert et al., 1994; Knowles, 1994; Kumar and Venkateswerlu, 1998; Miranda et al., 2001; Boncheva et al., 2006). Activated Cry toxin has been thought to bind with specific receptors (Ihara et al., 1998; Hua et al., 2001; Chen et al., 2005; Hernández and Ferré 2005), such as aminopeptidase N (APN) (Knight, et al., 1994; Martinez-Ramirez, et al., 1994; Sangadala, et al., 1994; Gill, et al.,

1995; Valaitis, et al., 1995) and cadherin-like protein (Vadlamudi et al., 1995; Ihara et al., 1998; Nagamatsu et al., 1998a; Nagamatsu et al., 1998b; Gahan et al., 2001; Gómez et al., 2001) locating on brush border membrane (BBM), and then the toxin molecule penetrates into the membrane after a certain conformational change (Rausell et al., 2004). Membrane inserted Cry toxin forms a tiny pore on BBM and disrupts effusion and influx of ions. Consequently, midgut epithelial cell looses homeostasis which leads to insect death (Ge et al., 1991; Walters et al., 1993; Schnepf et al., 1998; de Maagd, et al., 2001; Kato et al., 2006).

Cry toxin is constituted of three characteristic domains and each domain has peculiar function (Fig. 1, Li et al., 1991; Grochulski et al., 1995; Schwartz et al., 1997; Daniel et al., 2001).

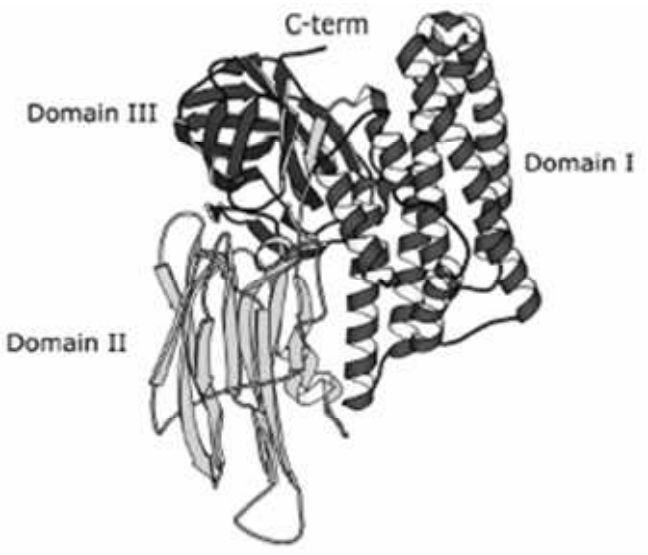

Fig. 1 3D model of Cry1Aa. Cry toxins including Cry1Aa and Cry1Ac have similar structure and are composed of three domains. This figure originates from Angsuthanasombat et al., 2004.

Domain I is composed of seven α-helices bundle and is thought to take a membrane insertion domain (Angsuthanasombat et al., 2004), and consequently it forms a pH-dependent pore or ion channel (Tran et al., 2001). Cry toxin can penetrate not only into the insect midgut cell and BBM vesicle (BBMV) prepared from the homogenate of insect midgut containing various proteins and lipids of epithelial cell membrane, but also into the liposome constituted of phosphatidylcholine and phosphatidylserine (Caroll et al., 1997; Kato et al., 2006). These results suggest that Cry toxin can moderately form a pore on artificial lipid bilayer without specific receptor(s) as well as the insect BBM. In addition, synthesized Cry1Ac α-4,5 helices that were 4^{th} and 5^{th} α-helices counted from N-terminus in domain I displayed pore forming activity (Gazit et al., 1994; Gerber and Shai, 2000). Supporting the result, it was reported that mutant of Cry1Ab N135Q, an amino acid residue in a center of α-4 helix, did not show pore forming activity to *M. sexta* BBMV (Tigue et al., 2001). These reports indicate that Cry1A toxin penetrates into the membrane by α-4,5 helices of domain I (Gazit et al., 1998). However, also other helices, α-2, 3, and 7 helices have been thought to involve in the pore formation (see **1.2. Introduction** in detail). On the other hand, it is known that Cry1Ab oligomerized into tetramer on *M. sexta* BBMV (Güereca and Bravo 1999; Rausell et al., 2004). Oligomerization was suggested to be vital for the pore formation activity of Cry toxin (Gómez et al., 2002b) and the activity may be sustained by α-5 helix (Gerber and Shai, 2000). The oligomerization activity was also observed in Cry4A and Cry4B which are the mosquitocidal Cry toxin (Kanintronkul et al., 2003; Pornwiroon et al., 2004). Amino acid sequence homology between Cry1Aa and Cry4 is only ~25%, suggesting assemblage of molecule may be common or highly conserved characteristic of all Cry toxin. On the basis of these previous works and on the investigation of colicin A, a α-helical pore forming toxin, Umbrella model is believed to be the membrane insertion and pore forming mechanism of Cry1A toxins (Fig. 2A, Knowles and Ellar., 1987; Duché et al., 1994; Gazit and Shai, 1995). In this model, tetramerized α-4, 5 helices of Cry1A toxin is supposed to insert into the BBM and forms a pore through negative charge of four aspartic acid residues on α-4 helix (Fig. 2B, Masson et al., 1999).

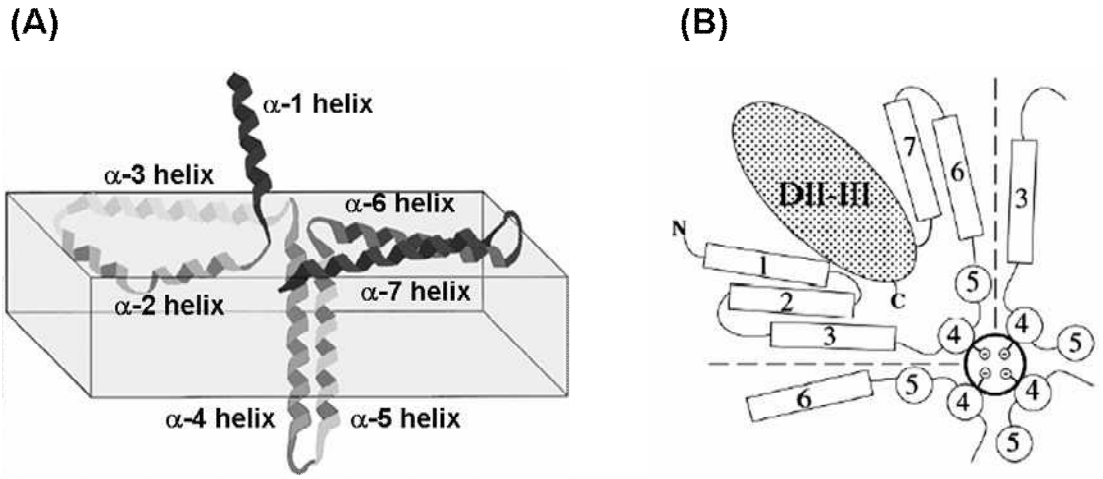

Fig. 2 Speculated membrane insertion and pore forming model of Cry toxin. (A) Umbrella model. In this model, it is believed that α-4, 5 helices insert into the membrane and the other helices spread on the membrane surface. This figure originates from Gazit et al., 1998 and was touched by the author of this doctoral thesis. (B) Pore forming model based on Umbrella model. α-4, 5 helices of tetrameric Cry toxin may form a pore, and the pore might be kept by negative charge derived from aspartic acid residues on α-4 helix. This figure originates from Masson et al., 1999.

Domain II is consisted of three antiparallel β-sheets including the receptor binding region (Lu et al., 1994; Rajamohan et al., 1996; Lee et al., 2000; Jurat-Fuentes et al., 2001). One of the evidence for interaction between the domain II and receptor binding is that recombinant domain II of Cry1C expressed by *E. coli* bound to *Spodoptera littoralis* BBMV and the binding was competed with Cry1C (Avisar et al., 2004). In the domain, several essential sites for receptor binding ability were reported. For instance, synthetic loop2 peptide corresponding to the region between β-6 sheet and β-7 sheet in the domain II prevented the binding of Cry1A toxins to Bt-R_1, one of the cadherin-like protein originates from *Manduca sexta* (see below this chapter) The hydropathic profile of Cry1Ab loop2 accommodated to Cry1A-binding region of Bt-R_1, indicating that the loop was suitable to bind with Bt-R_1 (Gómez et al., 2002a). In addition, loop2 correlated with APN binding as well as Bt-R_1 binding (Lee et al., 2000). Loop2 must be the key position for receptor binding of Cry1A toxins. In case of Cry11Aa which is the mosquito-specific Cry toxin similar to Cry4, synthesized loop-α8 peptide that is the loop structure between β-1 sheet and α-8 helix, and loop3 peptide corresponding to the loop between β-10 sheet and β-11 sheet strongly prevented the Cry11Aa binding to *Aedes aegypti* BBMV. E266 in the loop-α8 was crucial amino acid residue to be recognized by specific receptor on the *A. aegypti* BBMV. Loop2, however, had no binding inhibition activity against Cry1A toxins, showing the binding manner of Cry11Aa differed from that of Cry1A toxins (Fernández et al., 2005). Thus, the domain II concerns with the specific receptor binding on the insect midgut, but the mode of action is complex and the detail is yet to be solved.

Domain III is formed with two antiparallel β-sheets relating with insecticidal specificity, receptor binding (Schnepf et al., 1990; Daniel et al., 2002) and recognition of sugar side chain of glycoprotein (Knight et al., 1994). Domain III had GalNAc binding region on the outer surface of the domain (Burton et al., 1999) and the whole structure of domain III resembled cellulose binding domain of 1, 4-β-glucanase CenC derived from *Cellulomonas fimi* (Johnson et al., 1996; Murzin and Bateman 1997). These reports indicate that the domain III recognizes and interacts with oligosaccharide chain on the BBM. Actually, Cry1Ac binding ability of *M. sexta* BBMV and the 115

kDa APN was decreased by presence of GalNAc (de Maagd et al., 1999). But reducing of binding amount was not observed in Cry1Aa (Mason et al., 1995). It may reflect that domain III is the least similar domain between Cry1Aa and Cry1Ac, i.e., similarity is ~80%. On the other hand, interaction between APN and Cry1Ac was not inhibited by GlcNAc or galactose (de Maagd et al., 1999; Shitomi et al., 2006). This result revealed that the position of 4-hydroxyl group and 2-acetylamine group on sugar is essential for sugar recognition mechanism of domain III. In addition to the sugar recognition, domain III also determines the insecticidal specificity. Domain III swapping experiments showed that the domain may concern the specificity of insecticidal activity. For example, when domain III of Cry1Ab and Cry1Ac that had no insecticidal activity against *Spodoptera exigua* was exchanged for the domain of Cry1C that could kill the insect, the insecticidality of these hybrid toxins was augmented about 25 times (de Maagd et al., 2000). And furthermore, domain III of Cry1Ca and Cry1Fb which did not invest the toxicity against *Heliothis virescens* was converted into domain III of Cry1Ac which was highly toxic toward the insect, these heterogeneous Cry1Ca and Cry1Fb displayed 170 and 70 times toxicity compared to original toxin, respectively (Karlova et al., 2005). But Cry1Da and Cry1Ea did not express the toxicity even when the domain swapping was done. Moreover, a single report claims that Cry1Ac point-mutated in domain III has changed its binding ability to BBMV prepared from *M. sexta*, but not affecting the insecticidal activity (Burton et al., 1999), leaving domain III's real function as unclarified completely.

Specific receptor is one of the most important agents on Cry toxin interaction with insect BBM. A decade ago, several types of the receptor for Cry toxins were discovered from insect midgut. In earlier, aminopeptidase-N, APN, was identified as Cry1Ac receptor in *M. sexta* midgut (Knight et al., 1994). APN located on the surface of apical membrane of gut epithelial cell is a protease which can remove away neutral amino acid, leucine, alanine and others, from N-terminus. Some of the APN such as *M. sexta* 120 kDa APN are anchored on the membrane via glycosyl-phosphatidylinositol (GPI) anchor. (Garczynski and Adang, 1995) and have *N*- and *O*-linked sugar side chain (Oltean, et al., 1999). These sugar side chains are recognized by the domain III of Cry

toxin described below. Proceeding with the early report, many kinds of APN homolog have been found from various insects. Eight APN isoforms originated from five insects has demonstrated Cry toxin binding ability (Nakanishi et al., 2002); *B. mori* APN1 (Yaoi et al., 1999b), *M. sexta* APN1 (Knight et al., 1995), APN2 (Denolf et al., 1997), *H. virescens* 120-kDa APN (Gill et al., 1995), 170-kDa APN (Oltean et al., 1999), 110-kDa APN (Banks et al., 2001), *Lymantria dispar* APN1 (Garner et al., 1999) and *Epiphyas postvittana* APN (Simpson et al., 2000). APN-binding ability of Cry1A toxins was maintained by R368 and R369 residues on the loop2 of the domain II (Lee et al., 2000). Alternatively, the essential regions of *B. mori* 120 kDa APN which recognize Cry1Aa were identified as 135I-198P (Yaoi et al., 1999a). Immunolocalization analysis showed that Ms APN1 is localized on posterior midgut of *M. sexta* and it bound predominantly with Cry1Ac rather than Cry1Aa (Chen et al., 2005). In addition, artificial lipid monolayer composed of egg-yolk $_{L}$-α-phosphatidylcholine and *M. sexta* APN bound with Cry1Ac, and actually, Cry1Ac formed pore on the *M. sexta* BBMV containing APN and/or other receptor(s) (Cooper et al., 1998). Same inclinable result corresponding to Cooper's report was obtained from the experiment using *H. virescens* (Luo et al., 1997). All of these reports indicate cooperatively that APN is important for the interaction between Cry toxin and insect midgut. APN must be one of the suitable receptor proteins for insecticidal Cry toxin because APN is a kind of digestive protease which is a major common component of insect midgut.

As counterpart of APN, another Cry toxin receptor, cadherin-like protein (CadLP), was identified as Cry toxin receptor (Vadlamudi et al., 1995). Cadherin has repeatable ectodomain (EC) and is correlated with cell-cell adhesion (Ivanov et al., 2001). BT-R_1, one of the CadLP found from *M. sexta* midgut, possessed 12 ECs, and also had Cry1A toxins binding region on EC 11 (Dorsch et al., 2002). Not only BT-R_1, but also another CadLP, BtR_{175} originated from *B. mori*, OnBtR_1 derived from *Ostrinia nubilalis*, etc., were isolated from several insects (Nagamatsu et al., 1999; Flannagan et al., 2005). Compare to APN, CadLP shows low K_D value or high affinity to Cry1A toxin. In general, K_D value of APN is 100-1000 nM (Bravo et al., 2004; Shitomi et al., 2006), but that of CadLP is 1-100 nM (Jenkins and Dean, 2001; Dorsch et al., 2002; Xie rt al.,

2005). CadLP may capture Cry1A toxins precedent to APN in vivo. Bravo and her colleague proposed an interesting model for interaction between Cry toxins and BBM.

In their model, ①trypsinized or activated Cry toxin first, binds with CadLP on the BBM surface. ② Binding to CadLP triggers oligomerization of Cry toxin. ③ Oligomerized Cry toxin is then transferred to APN on the lipid raft that is the hydrophobic microdomain of lipid bilayer containing richly cholesterol, GPI-anchored protein and glycolipids (Sato, 2001; Bravo et al., 2004). Finally, oligomerized Cry toxin forms a pore on the BBM. However, cadherin operates in cell-cell adhesion, for that reason, cadherin must exist on the basolateral membrane or the border between cells. To interact with Cry toxin, CadLP has to be located in the exterior of epithelial cell membrane. Recently, localization of CadLP on the surface of the BBM was suggested in *H. virescens* and *M. sexta* (Aimanova et al., 2006). This report may be the evidence that the function of CadLP is not cell-cell adhesion.

In addition to these candidates of the reports, another binding proteins or receptor which are neither APN nor CadLP, were reported; i.e., alkaline phosphatase originated from *M. sexta* (Sangadala et al., 1994; McNall and Adang, 2003), P252 derived from *B. mori* (Hossain et al., 2004) and so on. P252 had a very high affinity toward Cry1A toxins (K_d value was 20-180 nM). Interestingly, it has been shown that P252 is the red fluorescent protein (RFP) that relates with antiviral activity on *B. mori* and has lipocalin repeat like chlorophylide binding protein (CBP) (Ganesh et al., 2007, unpublished data). Veritable role of this binding protein is still in an augment.

I focused on insecticidal and resistant machinery between Cry1Aa and Cry1Ac in my doctoral thesis. Because Cry1A toxins is one of the most widely used and investigated Cry toxins, and its toxicity is adapted to lepidopteran insect including many kinds of serious insect pests. *B. thuringiensis* and Cry toxin gene have been utilized worldwide for biopesticide and transgene for gene modified crops because of its order-specific insecticidal activity and non toxicity against vertebrate (Adamczyk et al., 2001; Burkness et al., 2001; Kumar and Kumar; Wan et al., 2004; ISAAA report., 2005; He et al., 2006). Biopesticide and transgenic crops are the most important tools for the integrated pest management that preserves environment and contributes to “sustainable

agriculture".

In this thesis, I investigated the membrane insertion region and pore forming model of Cry1Aa and Cry1Ac. As a result of Pronase digestion assay, a method to determine membrane inserted region of Cry1A toxins, it was clearly demonstrated that both of whole Cry1Aa and Cry1Ac molecules were protected by *B. mori* BBMV, namely? inserted into the BBMV, but the digestion pattern of Cry1Aa was different from Cry1Ac in detail as well as their oligomerization activity. And moreover, elucidation of Cry1Ac resistance mechanism on *Plutella xylostella* is also my aim. To measure galactose and GalNAc transferase activity between Cry1Ac susceptible *P. xylostella* and resistant one suggested that the mutation of the glycosyltransferase may trigger Cry1Ac resistance on *P. xylostella*. These two purposes are integrated into the question of why does a Cry toxin kill only target insect, while it's not inactive against the other one. If these are demonstrated, the knowledge must support to create unique transgenic Cry toxin which has a new insecticidal spectra and does not generate resistant insect.

Chapter 1

Determination of the membrane insertion region of Cry1Aa and the novel pore forming model

1.1. Abstract

Cry toxin produced by *Bacillus thuringiensis* demonstrates insecticidal activity by forming a pore on the brush border membranes (BBM) of midgut epithelial cells. Activated Cry1Aa or Cry1Ac bound to *Bombyx mori* BBM vesicle (BBMV) and free ones were digested vigorously by Pronase. These digests were compared by Western blotting using region-specific Cry1Aa antisera. Free Cry1Aa which has high toxicity towards *B. mori* excluded for α-2, 3 helices was digested completely at 2 mg/mL Pronase treatment, for 2.4 h at 37 ^{o}C. However, BBMV-bound Cry1Aa was very resistant to Pronase digestion. Domain I except α-1 helix remained in the BBMV and domain II and III also sedimented. Interestingly, a 15 kDa fragment was detected by only anti α-4, 5 antiserum. This fragment may be the dimer of α-4, 5 helices. Based on these results, Cry1Aa is thought to form a pore on two individual conformation; monomer and oligomer. On the other hand, Cry1Ac which does not kill *B. mori* displayed quite different digestion pattern. Free Cry1Ac including α-2, 3 helices was digested completely by 2 mg/mL treatment. Nevertheless, BBMV-bound Cry1Ac invested ultra-high protease resistance. All parts of Cry1Ac except the C-terminal region of domain III lingered tightly on the BBMV, suggesting that domain III C-terminus of Cry1Ac may be exposed on the membrane surface and other parts of Cry1Ac interact strongly with BBMV. Cry1Ac conformation on the BBM should differ widely from that of Cry1Aa.

1.2. Introduction

As described on **General introduction**, Umbrella model is believed to be the membrane insertion model of Cry toxin. In this hypothetical model, α-4, 5 helices is conceived to be the membrane insertion region and the remnant five α-helices are spread out on the membrane surface (Gazit et al., 1998). And then, oligomerization especially tetramerization may be substantial for pore formation (Fig. 2, Masson et al., 1999). However, it has been advocated based on the results of experiment using mutated Cry1A toxin and synthesized peptide. Only an amino acid replacement may affect whole conformation of Cry1A toxins, and more, synthesized peptide is 10 kDa at best; whose mass is < 1/5 as total molecular weight of Cry1A toxins, in other words, majority of the toxin is disregarded unreasonably. Indeed, several reports suggest that various parts of Cry1A toxin not only α-4, 5 helices must also be important in the toxicity and pore forming activity. For instance, Cry1Aa eliminated until α-2 helix decreased the toxicity compared to intact Cry1Aa (Ogiwara, et al., 1992). Moreover, Cry1Aa mutated at R99, E101, E116, E118 and D120 on α-3 helix had almost no pore forming activity (Vachon, et al., 2002), and P70G Cry1Ab mutated on α-2 helix also reduced the insecticidal activity without conformation change of the whole molecule (Arnold et al., 2001). Furthermore, hydrophobicity of α-7 helix plays an important role for the toxicity and pore forming activity. Recombinant Cry1Ac which exchanged the α-7 helix to the hydrophobic motif of diphtheria toxin, one of the pore forming toxin against mammalian cell (Greenfield et al., 1983), enhanced the insecticidality toward *Helicoverpa armigera* and pore forming activity (Chandra et al., 1999). Recently, it was reported that not only tetrameric Cry1Ab but also monomeric one, showed the toxicity and pore forming activity (Gómez et al., 2002b). These reports indicate Cry1A toxin does not require necessarily oligomerization to form a pore and all of the α-helices may relate with membrane insertion, namely, the membrane insertion model of Cry1A toxin and should not be only the Umbrella model.

I tried to advocate the membrane insertion and pore forming model of Cry1Aa and Cry1Ac using *Bombyx mori* BBMV. Cry1Aa is highly toxic against *B. mori* (Shunrei × Shogetu), but Cry1Ac displays no toxicity although its 85% homologous as Cry1Aa.

Nevertheless, both of toxins bind with *B. mori* BBMV proteins on native and denatured condition (Hossain et al., 2004; Shitomi et al., 2006). It strongly suggests that critical difference between Cry1Aa and Cry1Ac must be expressed following receptor binding stage. The strategy of my work to consider the supposition as shown below; first, activated Cry1Aa or Cry1Ac is mixed with *B. mori* BBMV and incubated. In the incubation time, Cry1A toxin binds to specific receptor(s) and interacts with the BBMV. Secondly, BBMV-bound Cry1Aa or Cry1Ac is treated by Pronase which is the mixture of very strong and non-specific protease originates from actinomycetes. As a result of the treatment, parts of Cry1A toxin on the BBMV surface must be digested, but membrane insertion or burying region should be degraded scarcely since these regions are protected by the lipid bilayer. Finally, digests of BBMV-bound Cry1A toxins are separated by SDS-PAGE and detected with Western blotting using region-specific Cry1Aa antisera. I named the methodology “Pronase digestion assay”. Elucidation of the membrane insertion region and pore forming mechanism between Cry1Aa and Cry1Ac is useful acquaintance for resolution of insecticidal and specificity mechanism on Cry toxin.

1.3. Material and Method

1.3.1. Insect and bacteria

B. mori hybrid Shunrei × Shogetsu larvae reared on artificial diet Silkmate (Nosan Kogyo, Yokohama, Japan) were used for the experiment. Cry1Aa and Cry1Ac were prepared from *B. thuringiensis* sotto T84A1 and *B. thuringiensis.* subsp. *kurstaki* HD-73, respectively.

1.3.2. Determination of protein concentration

Protein concentration was determined by Bio-Rad Protein Assay Dye Reagent Concentrate (Bio-Rad Lab, Hercules, CA, USA) using bovine serum albumin (BSA) as the standard.

1.3.3. Preparation of activated Cry1Aa and Cry1Ac

Preparation method of Cry1Aa and Cry1Ac was referred to the Suzuki's procedure (Suzuki et al., 1992). *B. thuringiensis* was cultured for 72 h in NYS medium at 30 °C on rotary shaker at 180 rpm and the incubated medium was centrifuged at 15,000 × *g* for 10 min at 4 °C. Precipitated bacteria was sonicated three times in 1 M NaCl at 20 kHz for 1 min with 30 second interval and recovered by centrifugation in the same condition described above. The precipitate was re-suspended by 1 M NaCl and double distilled water (DDW) each two times for washing and recovered by the centrifugation. This precipitate was regarded as ICP fraction, and then it was solubilized using 1.5 mL of 50 mM CAPS (pH 10) containing 100 mM NaCl and 10 mM DTT for 1 h at 37 °C on 180 rpm rotation. After solubilization, 100 μg/mL (final conc.) of trypsin was added to the suspension and incubated more at 37 °C for 1 h to prepare activated Cry1A toxin. The supernatant containing Cry1A toxin was recovered by 15,000 × *g* for 10 min at 4 °C. Finally, Cry1A toxin solution was diluted properly by 50 mM CAPS (pH 10) containing 100 mM NaCl. Cry1A toxins were not purified further, neutralized and frozen for stock to avoid conformation change and aggregation during these steps.

1.3.4. B. mori BBMV preparation

B. mori BBMV was prepared with the method of Wolfsberger et al., (1987). Two days-old 5^{th} instar larvae of *B. mori* placed on ice for anesthetization and then were extirpated for midgut. Midguts were homogenized in MET buffer (50 mM Tris-HCl, 300 mM mannitol, 5 mM EGTA, 12 mM $MgCl_2$, 1 mM PMSF, pH 7.4) and centrifuged for 2,500 × *g* for 15 min at 4 °C. The supernatant was centrifuged for 30,000 × *g* for 30 min at 4 °C, and the pellet was recovered and suspended into 50mM Tris-HCl (pH 7.4) containing 5mM EGTA. Finally, BBMV suspension was diluted to adjust the protein concentration to 5 mg/mL.

1.3.5. Preparation of antisera against various parts of Cry1Aa

Six parts of Cry1Aa were amplified by PCR using various primers (Fig. 3, Table 1) and the plasmid extracted from *B. thuringiensis sotto* T84A1 as template. PCR was done 40 cycles at 94 °C, 30 sec; 50-60 °C, 30 sec; 72°C, 30 sec, and the products were inserted into pET-35b (+) (Novagen, Madison, WI, USA) after digestion by *Bam*HI and *Xho*I. Each Cry1Aa fragment corresponding to amplified region was expressed as fusion protein with cellulose binding domain (CBD) in *E. coli* (BL21DE3) and pre-purified with $CB_{IN}D$ 200 Resin (Novagen) column chromatography. Subsequently, CBD tag was removed by Factor Xa (Promega, Madison, WI, USA) treatment and the separation of CBD and recombinant Cry1Aa fragment was done with SDS-PAGE using 15% polyacrylamide gel. After staining with coomassie brilliant blue, a part of the gel containing each recombinant Cry1Aa fragment were excised off and soaked into 1 % (w/v) SDS to extract the protein after homogenization. The extracts were powdered by freeze-drying, and the protein was precipitated by cold 90% (v/v) acetone at -30 °C overnight. The sedimented protein was recovered by centrifugation and suspended in a small amount of DDW. Purified peptide of Cry1Aa was injected into rabbit to immunize (~0.5 mg antigen/injection, injection was 4 or 5 times every other a week). At the beginning, α-1, 2, 3 helices-CBD was expressed and would be utilized for the antigen. But α-1,2,3 helices were unstable and digested easily after removal of CBD tag so I constructed α-2,3 helices-CBD.

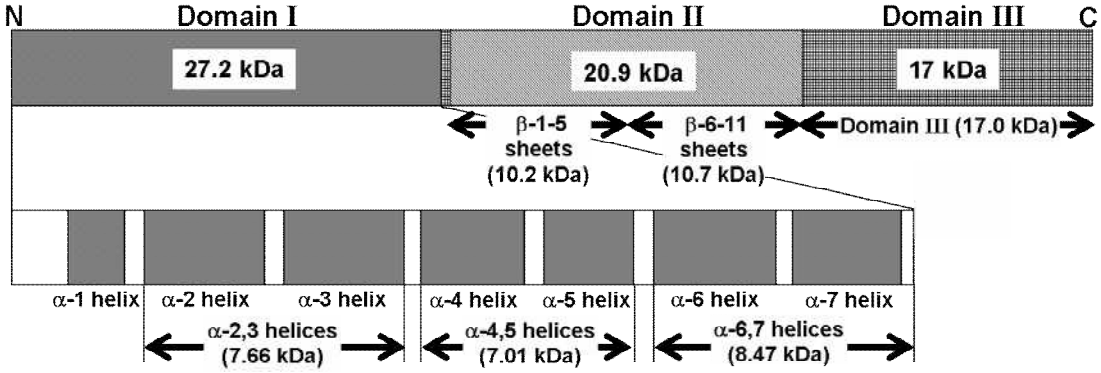

Fig. 3 Antigen region of the newly prepared, region- specific Cry1Aa antisera. Six parts of Cry1Aa were sub-cloned, expressed and used as the antigen. Arrowed regions were amplified by PCR, inserted into pET-35b (+), and expressed as fusion protein with cellulose binding domain (CBD). After removal of CBD, each part of Cry1Aa was purified and immunized to rabbit. Precise amino acid sequence of each region are shown as α-2, 3 helices: 54A-119A; α-4, 5 helices: 121P-182W; α-6.7 helices: 183G-253R; β-1-5 sheets; 266E-358F; β-6-11 sheets: 359R-455Q; Domain III; 463N-618R.

Table 1 Primer sequence for sub-cloning of each part of Cry1Aa

Cry1Aa part/section	5′primer	3′primer
α-2,3 helices/54A-119A	cgggatcctgctggatttgtgttagg	ccgctcgagtgcttcccactctctaa
α-4,5 helices/121P-182W	cgggatcctcctactaatccagcatta	ccgctcgagttaccaccttttgtccaaaca
α-6,7 helices/183G-253R	cgggatccgggatttgatgccgcgact	ccgctcgagttatcgactatcataatttg
β-1-5 sheets/266E-358F	cgggatccagaaatttatacgaaccca	ccgctcgagaaaaatccccaaaccag
β-6-11 sheets/359R-455Q	cgggatcctagaacattatcttcacc	ccgctcgagctgccaagaaaacgtt
domainⅢ/463N-618R	cgggatcctaatataattccttcatcac	ccgctcgagtctttctaaatcatattctg

1.3.6. SDS-PAGE and Western Blotting

SDS-PAGE was performed according to the Laemmli's method (Laemmli, 1970) using 7.5 or 15% gel with Protein Marker, Broad Range (2-212 kDa) (New England Biolabs, Beverly, MA, USA) or SIGAMAMARKER Low range size marker (Sigma-Aldrich, St Louis, MO, USA) as molecular weight standard. After SDS-PAGE, separated proteins were transferred to PVDF membrane, Hybond-P (GE Healthcare Bio-Sciences., Piscataway, NJ, USA), and overlaid with diluted first antiserum after blocking with PBST containing 1% (w/v) skim milk. Horseradish peroxidase (HRP)-conjugated IgG goat anti-rabbit F (ab')$_2$ (whole molecule; Cappel, Irvine, CA, USA) was used as secondary antibody. Detection was carried out using Enhanced Chemical Luminescence (ECL)/ Western Blotting Detection Reagents (GE Healthcare Bio-Sciences) and Hyperfilm ECL (GE Healthcare Bio-Sciences). Molecular mass of each protein band was determined by analytical software Quantity One (Bio-Rad Lab) as the average of four independent experiments per sample.

1.3.7. Dot blotting analysis to determine specificity of anti α-2,3 and α-6,7 antisera

Oligopeptide of α-3 helix, QAISRLEGLSNLYQIYAESFREWEA and α-6 helix, AATINSRYNDLTRLIGNYTDYAVRW were synthesized and 5 μg of each was blotted onto Hybond-P. More four dots were spotted on the membrane with the oligopeptides sequentially diluted two-fold. Anti α-2, 3 or α-6, 7 antisera were utilized to detect. As a negative control, each spot was detected with the secondary antibody alone.

1.3.8. Pronase digestion of free Cry1Aa or Cry1Ac

Activated Cry1Aa or Cry1Ac (2.5 μg = 40 pmol) in 10 μL aqueous solution was mixed with 5 μL of 5 mg/mL BSA dissolved in 50 mM Tris-HCl (pH 7.4) containing 5 mM EGTA and incubated for 30 min at 25 °C. BSA was added for corresponding to the substrate concentration of BBMV-bound Cry1A toxin digestion. Then, 3.75 μL of 0.5-10 mg/mL Pronase solution containing 100 mM calcium acetate and 0.5% (w/v) NaN_3 was added. Final concentration of Pronase was 0.1 to 2 mg/mL. Digestion was performed for 2.4 h at 37 °C and the reaction was stopped by addition of SDS-PAGE sample buffer with boiling at 95 °C for 3 min. The digests were separated by SDS-PAGE using 15% gel and detected with Western blotting using region-specific Cry1Aa antisera. In this experiment, BSA and Pronase solution was prepared every time and the leftovers were never used again.

1.3.9. Pronase digestion of BBMV-bound Cry1Aa or Cry1Ac

Activated Cry1Aa or Cry1Ac (25 μg or 400 pmol) in 100 μL aqueous solution and 50 μL of 5 mg protein/mL *B. mori* BBMV suspension were mixed and incubated for 30 min at 25 °C. After incubation, 37.5 μL of 5-10 mg/mL Pronase solution containing 100 mM calcium acetate and 0.5 % (w/v) NaN_3 was added to adjust to a final concentration of 1-2 mg/mL Pronase. Reaction was done for 24 h at 37 °C. After reaction, the mixture was centrifuged at 15,000 × *g* for 15 min at 4 °C, and the precipitate was rinsed three times with 50 mM Tris-HCl (pH 8.3) containing 150 mM NaCl. The final precipitate was resolved by SDS-PAGE using 15% gel, and the proteins were analyzed by Western blotting described above (Fig. 4).

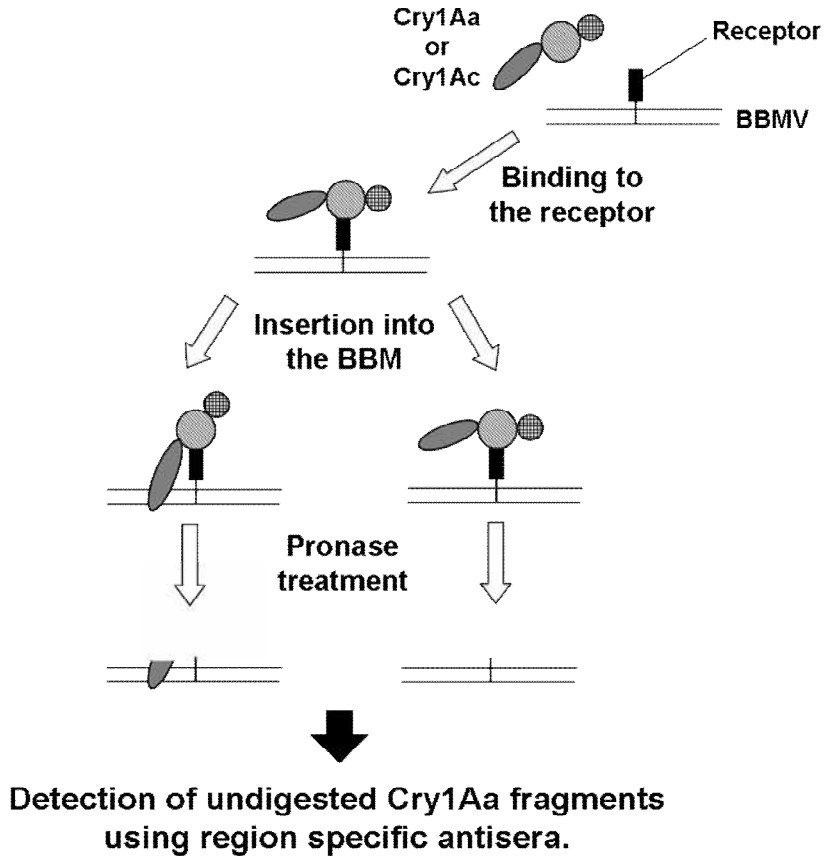

Fig. 4. Schematic principle of Pronase digestion assay. For the experimental detail, see **1.2. Introduction** and *1.3.9. Pronase digestion of BBMV-bound Cry1Aa or Cry1A.*

1.3.10. Oligomerization assay of Cry1Aa and Cry1Ac

Hundred μL of 0.5 μM activated Cry1Aa or Cry1Ac and 50 μL of 5 mg protein/mL *B. mori* BBMV suspension were mixed and incubated for 1 h at 25 °C. After incubation, the mixture was centrifuged at 15,000 × *g* for 20 min at 4 °C and Cry1A toxin bound BBMV was recovered. The BBMV was washed twice with 50 mM Tris-HCl (pH 8.3) containing 150 mM NaCl to remove unbound Cry1A toxin. Washed BBMV was solubilized by solubilization buffer (50 mM Tris-HCl, 150 mM NaCl, 1% (v/v) Triton X-100, pH 8.3) on ice for 1h. After solubilization, solubilized and insolubilized fractions were separated by centrifugation at 100,000 × *g* for 30 min at 4 °C. Insolubilized fraction was washed with solubilization buffer. These two fractions were denaturated by SDS-PAGE sample buffer at 60 °C or 95 °C for 3 min. Twenty μL of 0.5 μM activated Cry1Aa or Cry1Ac mixed with 10 μL of 5 mg/mL BSA was incubated for 1h and denaturated similarly for a control (Fig. 5). All samples were separated by SDS-PAGE using 7.5% gel and detected by anti Cry1Aa antiserum or anti Cry1Ac antiserum.

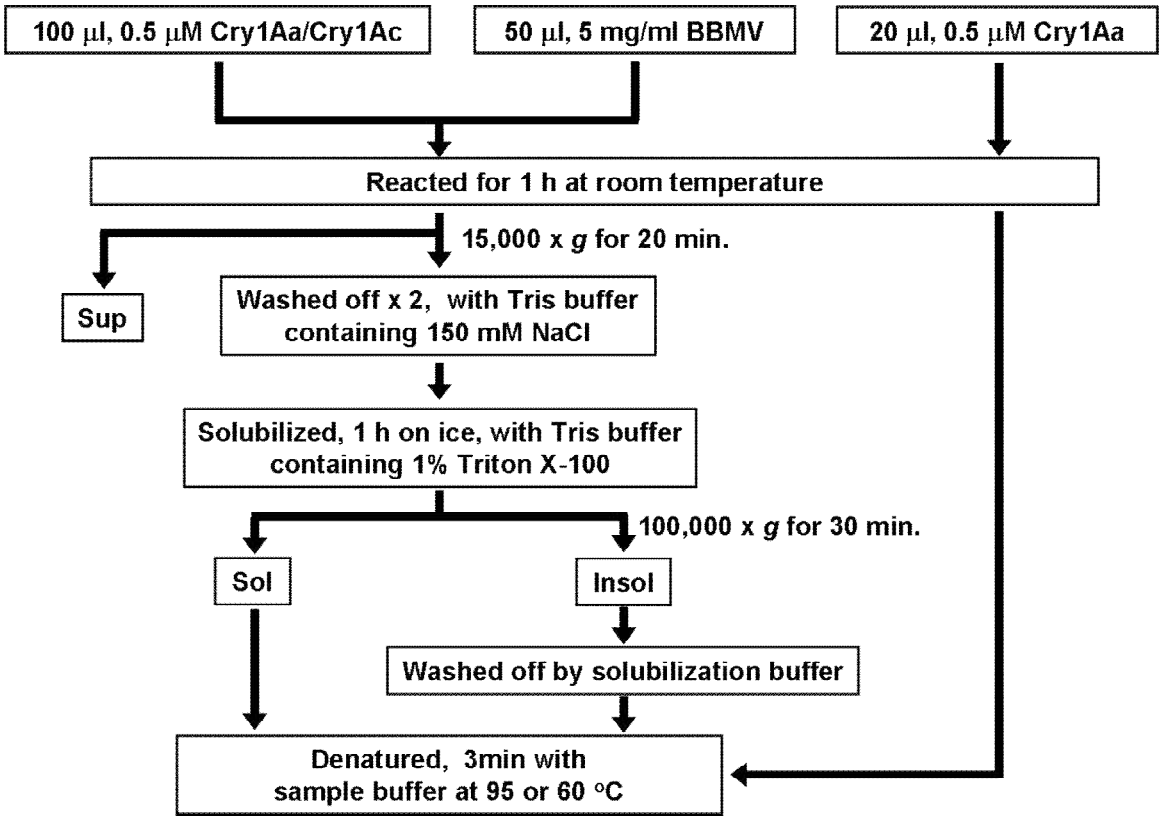

Fig.5. Flowchart of oligomerization assay. For the experimental detail, see *1.3.10. Oligomerization assay of Cry1Aa and Cry1Ac.*

1.4. Result

1.4.1. Specificity of region-specific Cry1Aa antisera

Specificity of region-specific Cry1Aa antisera was checked by Western blotting (Fig. 6). All antisera had high specificity and did not show non-specific binding to *B. mori* BBMV protein. Consequently, all of these antisera were used to detect the Cry1A toxins digests.

Moreover, anti α-2, 3 and α-6, 7 antisera were able to detect α-3 and α-6 helices, respectively (Fig. 7).

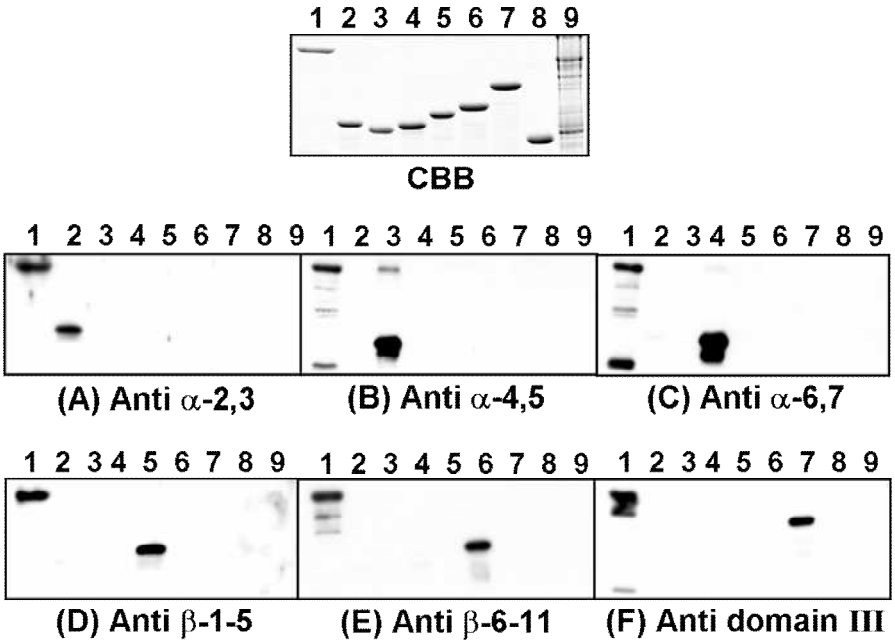

Fig.6. Specificity test of region-specific Cry1Aa antisera. Specificity of these antisera was checked by Western blotting. Five μg of each antigens were blotted onto PVDF membrane and detected by anti α-2, 3 antiserum (Panel A), anti α-4, 5 antiserum (B), anti α-6,7 antiserum (C), anti β-1-5 antiserum (D), anti β-6-11 antiserum (E), or anti domain III antiserum (F). The uppermost panel is the result of CBB staining. Lane 2; α-2,3-CBD, lane 3; α-4,5-CBD, lane 4; α-6,7-CBD, lane 5; β-1-5-CBD, lane 6; β-6-11-CBD, lane 7; Domain III-CBD. Lane 1 is Cry1Aa as positive control, lanes 8 and 9 are CBD and *B. mori* BBMV as negative control, respectively.

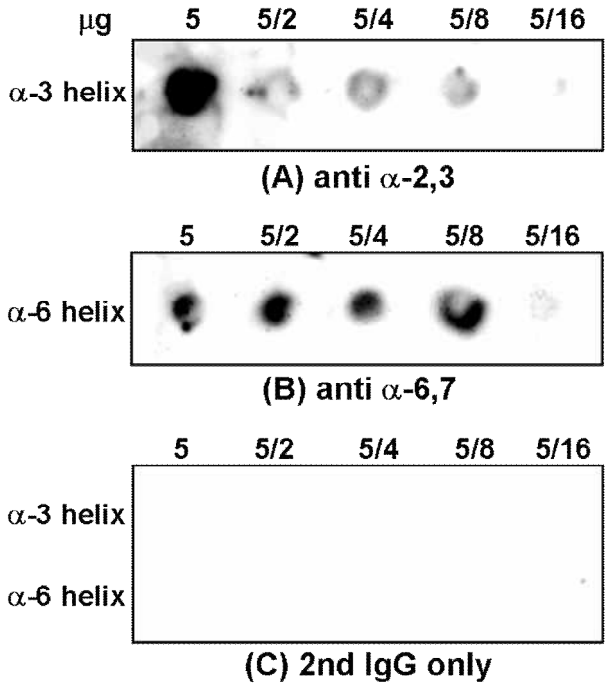

Fig.7. Detailed specificity test of anti α-2, 3 and α-6, 7 antisera. All panels are results of dot blotting analysis. Five μg of synthesized α-3 or α-6 helix and sequentially two times diluted four spots were blotted onto PVDF membrane. Each spot was detected by dot blotting with anti α-2, 3 antiserum (Panel A), anti α-6, 7 antiserum (B) or secondary IgG alone (C). Numbers above each spot represents amount of blotted peptide.

1.4.2. Pronase digestion of free Cry1Aa

Free or aqueous Cry1Aa was digested efficiently by Pronase (Fig. 8). Full-length Cry1Aa was not detected even at 0.1 mg/mL Pronase treatment for 2.4 h (Fig. 8, lane 2 on all panels). α-4, 5 and α-6, 7 helices were digested completely at 2 mg/mL treatment (Fig. 8B and C, lane 6), but α-2, 3 helices was recognized clearly on the treatment (Fig. 8A, lane 6).

Domain II, β-1-5 and β-6-11 sheets, and domain III were more fragile than domain I against protease. Pronase treatment of 0.5 mg/mL was enough to digest these regions entirely (Fig. 8D, E and F, lane 4).

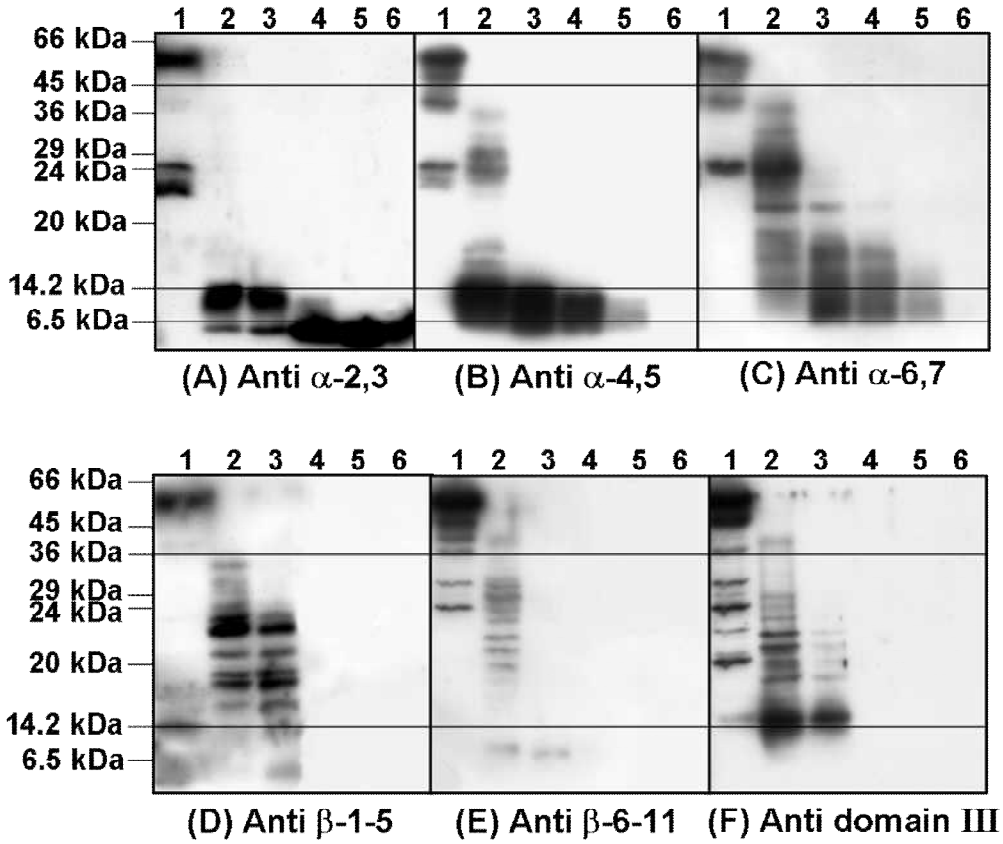

Fig.8. Pronase digestion of free Cry1Aa. Two point five μg (40 pmol) of free Cry1Aa containing 25 μg BSA in 15 μL were digested by Pronase from 0.1 to 2 mg/mL at 37 °C for 2.4 h. Digests were detected by Western blotting using anti α-2,3 antiserum (Panel A), anti α-4,5 antiserum (B), anti α-6,7 antiserum (C), anti β-1-5 antiserum (D), anti β-6-11 antiserum (E) or anti domain III antiserum (F). Lane 1: non-treated free Cry1Aa; lane 2: 0.1 mg/mL Pronase digests; lane 3: 0.2 mg/mL Pronase digests; lane 4: 0.5 mg/mL Pronase digests; lane 5: 1 mg/mL Pronase digests; lane 6: 2 mg/mL Pronase digests.

1.4.3. Pronase digestion of BBMV-bound Cry1Aa

BBMV-bound Cry1Aa was not degraded effectively compared to free Cry1Aa (Fig. 9). Full-length Cry1Aa was detected faintly at 1 mg/mL Pronase treatment for 24 h that of Pronase concentration and the reaction time is ten times as free Cry1Aa digestion (Fig. 9B and C, lane 2). Anti α-4, 5 and α-6, 7 antisera recognized 30-35 kDa fragments but anti α-2, 3 antiserum did not (Fig. 9A, B and C, lane 2-5). Instead of these fragment, anti α-2, 3 antiserum detected a 7.5 kDa peptide (Fig. 9A, lane 2-6). Interestingly, only anti α-4, 5 antiserum detected a 15 kDa fragment (Fig. 9B, lane 2-6).

Alternatively, β-6-11 sheets and domain III remained as a 30 kDa fragment (Fig. 9E and F, lane 2-5). However, almost no fragments were recognized by anti β-1-5 antiserum (Fig. 9D).

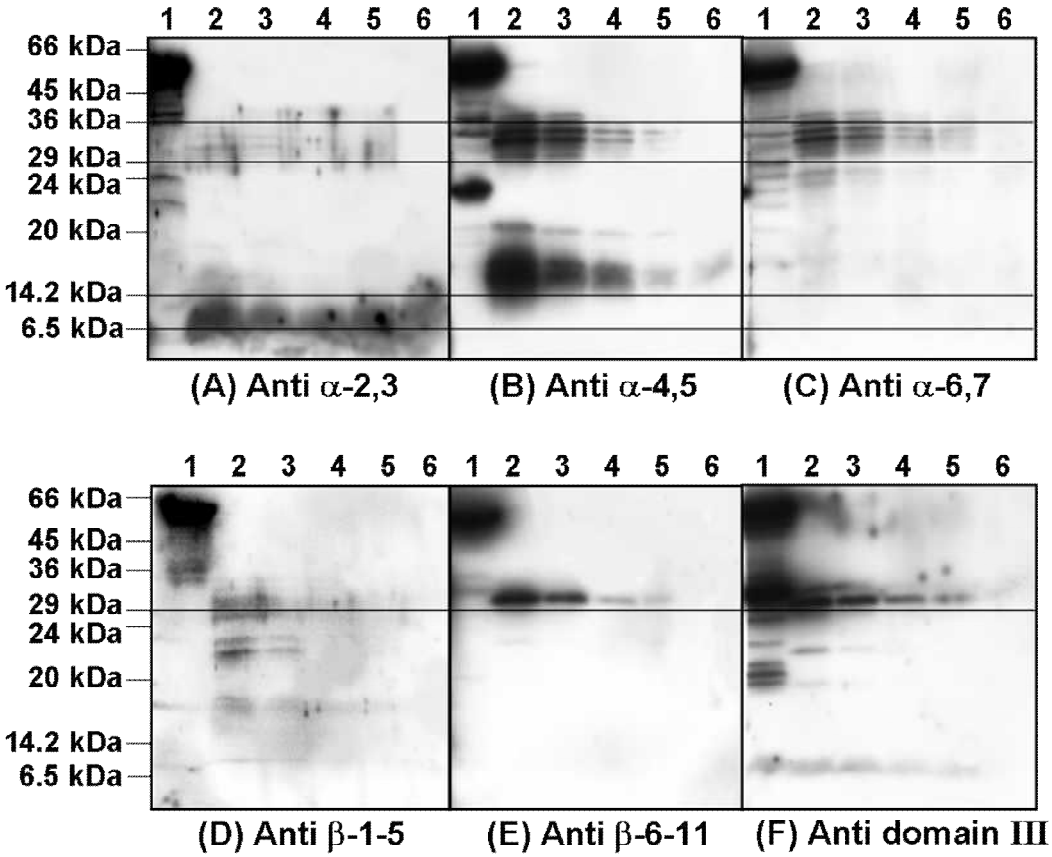

Fig.9. Pronase digestion of BBMV-bound Cry1Aa. One hundred μL of 250 μg/mL Cry1Aa and 50 μL of 5 mg protein/mL *B. mori* BBMV were mixed and incubated for 30 min. Then, Pronase was added to the mixture range from 1 to 2 mg/mL and reacted at 37 °C for 24 h. After digestion, Cry1Aa fragments binding with BBMV was recovered by centrifugation at 15,000 × *g* for 20 min and detected by Western blotting using anti α-2,3 antiserum (Panel A), anti α-4,5 antiserum (B), anti α-6,7 antiserum (C), anti β-1-5 antiserum (D), anti β-6-11 antiserum (E) or anti domain III antiserum (F). Lane 1: non-treated BBMV-bound Cry1Aa; lane 2: 1 mg/mL Pronase digests; lane 3: 1.25 mg/mL Pronase digests; lane 4: 1.5 mg/mL Pronase digests; lane 5: 1.75 mg/mL Pronase digests; lane 6: 2 mg/mL Pronase digests.

1.4.4. Pronase digestion of free Cry1Ac

Result of free Cry1Ac digestion demonstrated similar manner to free Cry1Aa but it was degraded readily rather than Cry1Aa (Fig. 10). Cry1Ac fragments were no longer detected at 0.5 mg/mL Pronase treatment in case of anti α-4, 5 and α-6, 7 antisera detection (Fig. 10B and C, lane 4). Even in α-2, 3 helices, it was almost digested at 2 mg/mL treatment (Fig. 10A, lane 6).

On the other hand, domain II and III were decomposed quickly compared to domain I; these domains were digested completely at 0.1 mg/mL treatment (Fig. 10E and F, lane 2).

Anti β-1-5 antiserum could not detect full length Cry1Ac as well as its digests (Fig. 10D). It may be the reason that anti β-1-5 antiserum was raised from Cry1Aa β-1-5, therefore, the specificity of anti β-1-5 antiserum may not accommodate to Cry1Ac β-1-5 sheets.

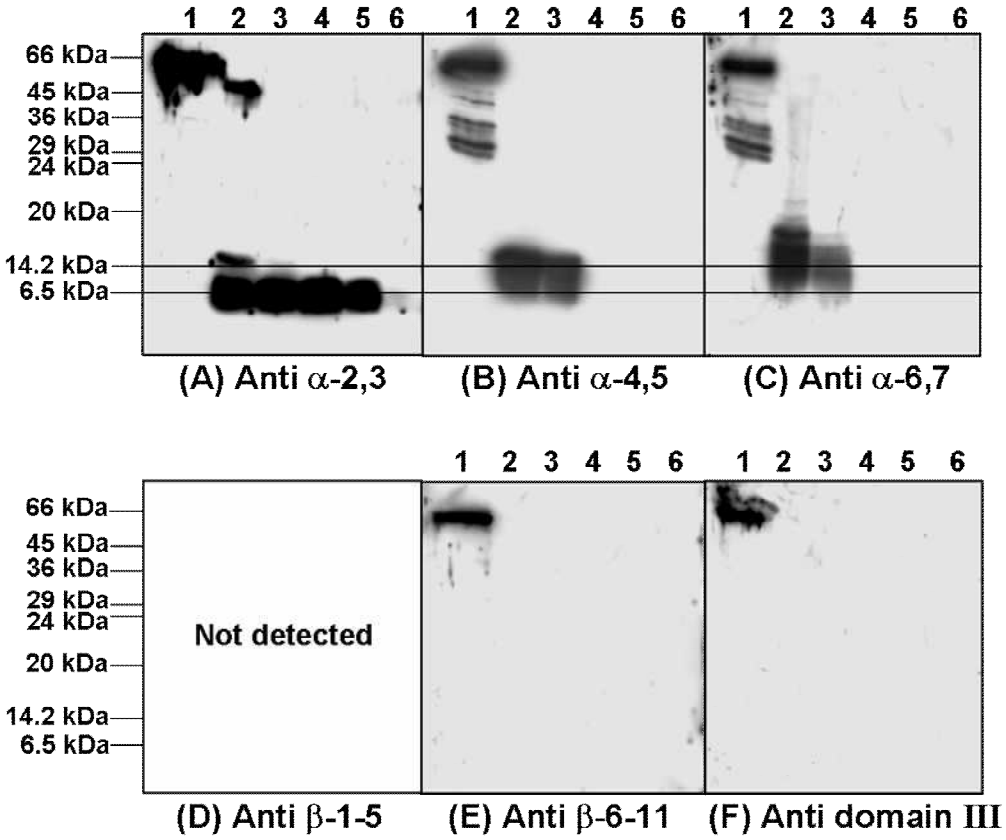

Fig.10. Pronase digestion of free Cry1Ac. Sample preparation and detection method was same as "Pronase digestion of free Cry1Aa" except Cry1Ac was used instead of Cry1Aa. Panel (A) is the result of anti α-2,3 antiserum detection; (B) anti α-4,5 antiserum; (C) anti α-6,7 antiserum; (D) anti β-1-5 antiserum; (E) anti β-6-11 antiserum; (F) anti domain III antiserum. Lane 1: non-treated BBMV-bound Cry1Ac; lane 2: 0.1 mg/mL Pronase digests; lane 3: 0.2 mg/mL Pronase digests; lane 4: 0.5 mg/mL Pronase digests; lane 5: 1 mg/mL Pronase digests; lane 6: 2 mg/mL Pronase digests.

1.4.5. Digestion of BBMV-bound Cry1Ac with Pronase

BBMV-bound Cry1Ac displayed extremely protease tolerance in contrast to Cry1Aa. Digestibility of all Cry1Ac fragments did not proportionate to Pronase concentration (Fig. 11). A 53 kDa fragment which was nearly full-length Cry1Ac appeared on the detection of anti α-4,5 and α-6,7 antisera, moreover, 26-31 kDa fragments were also recognized by these antisera (Fig. 11B and C, lane 2-6). While, anti α-2, 3 antiserum detected only <6.5 kDa peptide similar to Cry1Aa digestion (Fig. 11A, lane 2-6).

On the other hand, anti β-6-11 antiserum bound to a 24 kDa fragment but anti domain III antiserum was not. In addition, both of antisera recognized presumably common 6.5 kDa peptide (Fig. 11E and F, lane 2-6).

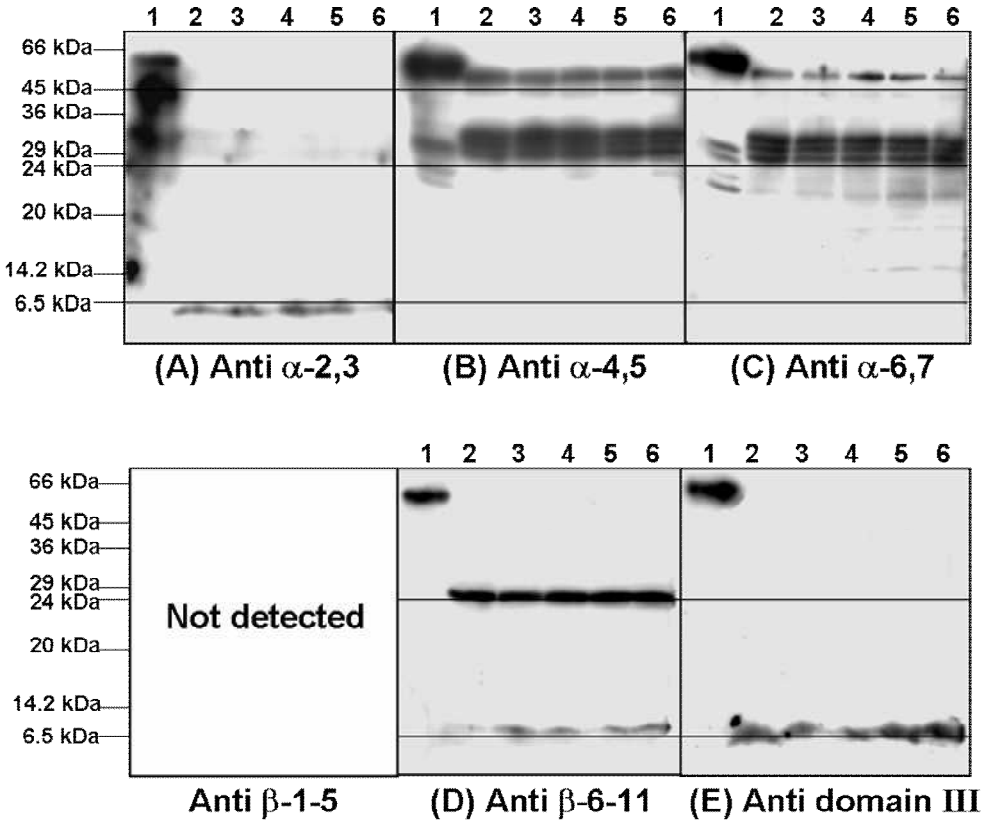

Fig.11. Pronase digestion of BBMV-bound Cry1Ac. Sample preparation and detection method was the same as "Pronase digestion of BBMV-bound Cry1Aa" except Cry1Ac was used instead of Cry1Aa. Panel (A) is the result of anti α-2,3 antiserum detection; (B) anti α-4,5 antiserum; (C) anti α-6,7 antiserum; (D) anti β-1-5 antiserum; (E) anti β-6-11 antiserum; (F) anti domain III antiserum. Lane 1: non-treated BBMV-bound Cry1Ac; lane 2: 1 mg/mL Pronase digests; lane 3: 1.25 mg/mL Pronase digests; lane 4: 1.5 mg/mL Pronase digests; lane 5: 1.75 mg/mL Pronase digests; lane 6: 2 mg/mL Pronase digests.

1.4.6. Oligomerization assay of Cry1Aa and Cry1Ac

Oligomerization activity between Cry1Aa and Cry1Ac was quite different (Fig. 12). Tetrameric Cry1Aa was formed on both 1% (v/v) Triton X-100 solubilized fraction and the insolubilized fraction (Fig. 12A, Sol. and Insol., lane 2), but monomeric Cry1Aa was not detected on solubilized fraction (Fig. 12A, Sol., lane 2). Interestingly, Cry1Aa also formed tetramer without BBMV (Fig. 12A, Without BBMV, lane 2). The tetramer was dissociated by boiling at 95 °C with SDS-PAGE sample buffer. On the other hand, Cry1Ac oligomerized neither through incubation with BBMV nor without one (Fig. 12B).

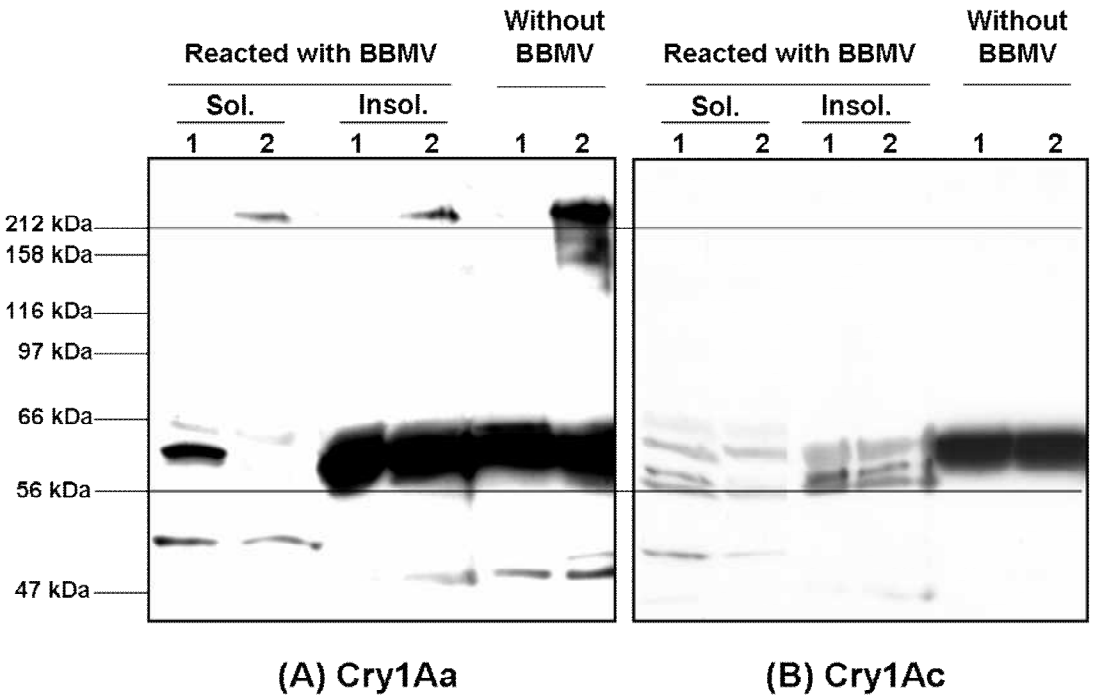

Fig. 12 Oligomerization assay of Cry1Aa and Cry1Ac. Hundred μL of 0.5 μM activated Cry1Aa or Cry1Ac and 50 μL of 5 mg protein/mL *B. mori* BBMV were mixed and incubated for 1 h at 25 °C. After incubation, BBMV-bound Cry1A toxin was recovered by centrifugation at 15,000 × *g* for 20 min and washed out using Tris buffer containing 150 mM NaCl. Washed BBMV was solubilized with 1% (v/v) Triton X-100 on ice for 1h, and the solubilized (Sol.) and insolubilized (Insol.) fraction was separated by centrifugation at 100,000 × *g* for 30 min. (A) Cry1Aa; (B) Cry1Ac. Lane 1: Denaturated by SDS-PAGE sample buffer at 95 °C for 3 min; lane 2: Denaturated by the buffer at 60 °C for 3 min.

1.5. Discussion

1.5.1. Pronase digestion of free Cry1Aa

Digestibility of free Cry1Aa differed widely on the each domain. Antisera recognized each part of domain I, α-2,3, α-4,5 and α-6,7 helices, detected 6.5 kDa fragment at minimum (Fig. 8A, B and C). These fragment were α-2, 3, α-4, 5, and α-6, 7 helices itself respectively since the molecular weight, 6.5 kDa, is nearly equal to each α-helices. On the detection of anti α-2, 3 and α-4, 5 antisera, common 14 kDa fragment was observed (Fig. 8A and B, lane 2 and 3). The 14 kDa fragment is thought to be α-2-5 helices based on the same logic described above. As described on **1.2. Introduction**, domain I is the most essential domain to form a pore for Cry toxins, therefore, it is important that domain I invests high protease resistance to antagonize against proteases secreted from insect midgut. Interestingly, α-2, 3 helices showed the highest protease resistance (Fig. 8A, lane 6), indicating α-2, 3 helices undertake an important role on the pore formation. Indeed, an indication about the significance of α-3 helix activity on the pore formation was reported (Vachon et al., 2002).

Alternatively, domain II and III were slightly contrasted to domain I. These domains were digested completely at 0.5 mg/mL treatment (Fig. 8D, E and F, lane 4). Domain II and III are composed mostly of β-sheets, reversely, domain I is constructed by α-helix only. The diversity of secondary and tertiary structure among these domains should affect stability against protease.

Hypothetical digestion pattern of free Cry1Aa is summarized in Fig. 13. First, α-1 helix may be removed from full-length Cry1Aa since α-1 helix is supposed to trim off easily in activation process of the protoxin (Gómez et al., 2002b). Cry1Aa having no Cry1Aa divides into 14 kDa and ~40 kDa fragments; the former is α-2-5 helices and this is the C-terminal region from α-6 helix. Afterwards, 14 kDa fragment is halved into α-2, 3 helices (<10 kDa) and α-4, 5 helices (<10 kDa), and ~40 kDa fragment is also cloven into two ~20 kDa fragments. One of the two ~20 kDa fragments containing α-6 helix gradually gets degraded to α-6, 7 helices, and the other including domain III was digested quickly. Finally, all fragments except α-2, 3 helices are digested completely.

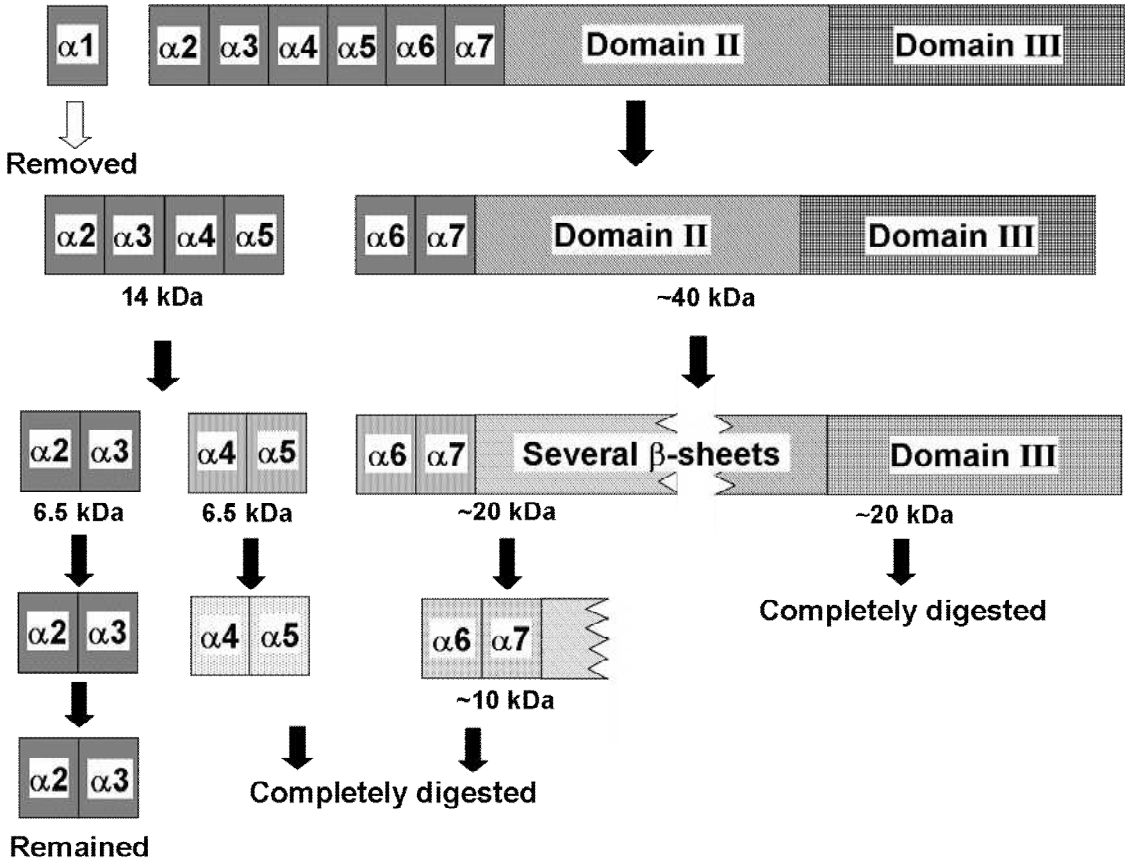

Fig. 13 Supposed flow chart of free Cry1Aa fragmentation by Pronase. First, α-1 helix was removed and α-2-5 helices (14 kDa) were excised from domain I. α-6,7 helices within domain II and III (~40 kDa) were gradually digested to α-6,7 helices. On the other hand, α-2-5 helices were divided into α-2, 3 helices (6.5 kDa) and α-4, 5 helices (6.5 kDa) at the loop structure between α-3 and α-4 helix. Despite vigorous digestion, α-2, 3 helices remained till the last.

1.5.2. Digestion of BBMV-bound Cry1Aa with Pronase

BBMV-bound Cry1Aa was difficult to digest compared to free one. It was not digested perfectly although 1 mg/mL Pronase treatment for 24 h. Several fragments of 30-35 kDa were detected by anti α-4,5 and α-6,7 antisera but not by anti α-2,3 antiserum (Fig. 9A, B and C, lane 2-5). Instead of these fragments, anti α-2, 3 antiserum detected a 7.5 kDa peptide which was presumed for α-2, 3 helices itself based on the molecular weight (Fig. 9A, lane 2-6). All of these fragments may be inserted into the BBMV without gradual segmentation because no intermediate fragment generated by endo-digestion was detected (Fig. 9 all panels, and refer Fig. 4). Especially, a 7.5 kDa peptide thought to be α-2, 3 helices was not digested anymore from 1 to 2 mg/mL digestion. α-2, 3 helices of BBMV-bound Cry1Aa exhibited the highest stability against protease. These results revealed that domain I is quite stable against protease attack for tight insertion into the BBMV.

Interestingly, a 15 kDa fragment was detected by anti α-4, 5 antiserum alone (Fig. 9B, lane 2-6). This fragment did not originate from 30-35 kDa fragments because 15 kDa and 30-35 kDa fragments were observed simultaneously at the same intensity. Anti α-2, 3 and α-6, 7 antisera could not detect the fragment although these antisera could recognize the neighboring region of α-4, 5 helices. However, molecular weight of α-4, 5 helices is only ~7 kDa, it is speculated that the 15 kDa fragment includes α-3 helix and α-6 helix at least. Result of the specificity test for antisera demonstrated that anti α-2, 3 and α-6, 7 antisera recognized α-3 and α-6 helices, respectively (Fig. 7A and B). If the 15 kDa fragment comprises α-3 helix and α-6 helix, it should be detected with both of anti α-2, 3 and α-6, 7 antisera, but the fragment was not detected actually by these antisera. For that reason, the 15 kDa fragment might not include α-3 helix and α-6 helix and it would be dimer of α-4,5 helices. In fact, it was reported that synthesized α-4, 5 helices oligomerized spontaneously by itself (Gerber et al., 2000). In conclusion, i suggest that Cry1Aa inserts into the membrane and forms a pore in two forms; one as monomer, and the other is tetramer (describe in detail available at *1.5.6. Hypothesized membrane insertion and pore forming model of Cry1Aa*).

On the other hand, C-terminal half of Cry1Aa, β-6-11 sheets of domain II and domain

III, was also hardly digested. A common 30 kDa fragment was detected by anti β-6-11 and domain III antisera (Fig. 9E and F, lane 2-5). This fragment may be buried into the membrane similar to domain I. In contrast, β-1-5 sheets, N-terminal half of domain II, was degraded readily in comparison when compared with other parts of Cry1Aa (Fig. 9D). This result means that β-1-5 sheets must be exposed on the BBM surface.

Supposed digestion pattern of BBMV-bound Cry1Aa is summarized in Fig. 14. On monomeric Cry1Aa, α-1 helix may first be removed from full-length Cry1Aa, and α-1 helix lacked Cry1Aa is divided at center of β-1-5 sheets into 35 kDa and 30 kDa fragments. Former 35 kDa fragment corresponding to N-terminal half of Cry1Aa is fragmented more into α-2, 3 helices (7.5 kDa) and another 30 kDa fragment including α-4-7 helices with a part of β-1-5 sheets. Both of 30 kDa fragments are degraded without intensive digestion, and all fragments excluding α-2, 3 helices are removed from the BBMV. Meanwhile, tetrameric Cry1Aa may be digested completely except dimeric α-4, 5 helices (15 kDa). α-4, 5 dimer might have originated from the tetrameric one. Perhaps, α-4,5 tetramer is separated into the dimer by Pronase digestion or sample denaturation step for SDS-PAGE.

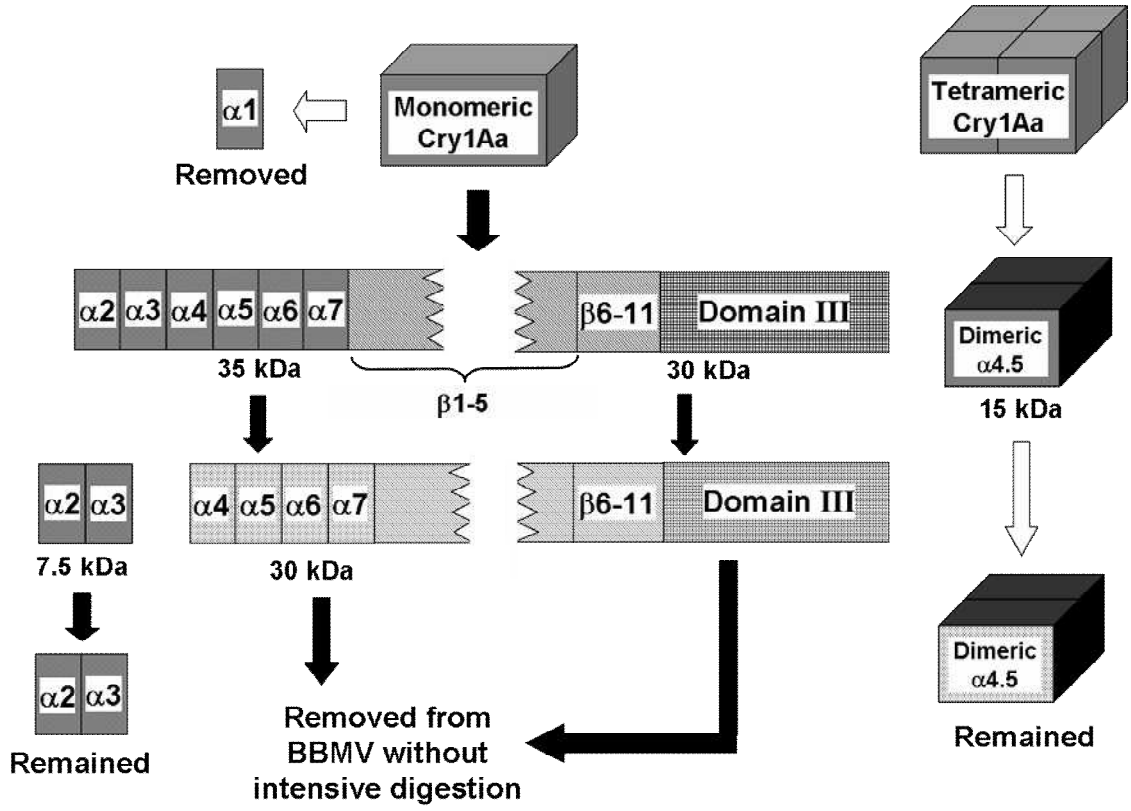

Fig. 14 Summarized fragmentation scheme of BBMV-bound Cry1Aa on the digestion of Pronase. In the initial stage of digestion, α-1 helix was trimmed off. Then, BBMV-bound Cry1Aa was segmented into two portions; one was the fragment from α-2 helix to N-terminal of β1-5 sheets (35 kDa), another was domain III with C-terminal half of domain II (30 kDa). A 35 kDa fragment was further split into a α-2, 3 helices (7.5 kDa) and the fragment range from α-4 helix to N-terminal of β1-5 sheets (30 kDa). Both of 30 kDa fragments gradually disappeared without further fragmentation, but α-2,3 helices remained in the BBMV. Alternatively, 15 kDa fragment corresponding to dimeric α-4,5 helices was generated from oligomeric Cry1Aa which was thought to be tetramer especially, and the fragment also remained faintly even う with strong Pronase digestion.

1.5.3. Pronase digestion of free Cry1Ac

Digestion pattern of free Cry1Ac was similar to Cry1Aa but not identical. About 6.5-10 kDa fragment was detected by anti α-2,3, α-4,5, and α-6,7 antisera, respectively (Fig. 10A, B and C). These fragments must be each α-helices itself. In addition, a 14 kDa fragment was recognized by anti α-2,3 and α-4,5 antisera (Fig. 10A and B, lane 2 and 3). Same fragment was observed on free Cry1Aa digestion. These results indicate that the digestion pattern between free Cry1Aa and Cry1Ac is basically same. However, domain I of free Cry1Ac was fragmented readily rather than that of Cry1Aa; 0.5 mL Pronase treatment was enough to digest full length Cry1Ac and the fragment (Fig. 10B and C, lane 4). Also α-2,3 helices that had the highest protease tolerance was digested completely at 2 mg/mL treatment (Fig. 10A, lane 6).

On the other hand, domain II and III were more fragile against protease than domain I. No fragment derived from these domains was detected by anti β-6-11 and domain III antisera even with 0.1 mg/mL Pronase treatment (Fig. 10E and 11F, lane 2). All of these results indicate that free Cry1Ac especially domain II and III is digestable contrast with free Cry1Aa. Resemblance of the digestion pattern between Cry1Aa and Cry1Ac must be result of the similarity in highly molecular conformation of the toxins. However, Cry1Ac fragility suggests that these molecular structures are not identical completely each other. It could be remarkably different in domain II and III.

Flow chart of supposed digestion manner on free Cry1Ac is shown on Fig. 15. α-1 helix and C-terminal half may be removed or digested quickly. The remnant is separated into α-2-5 helices (14 kDa) and α-6 helix including part of β-1-5 (<20 kDa). Fourteen kDa fragment is split to α-2,3 helices (6.5 kDa) and α-4,5 helices (~10 kDa). In addition, also <20 kDa fragment is digested to α-6,7 helices (~10 kDa), and finally, all of these fragments are digested completely.

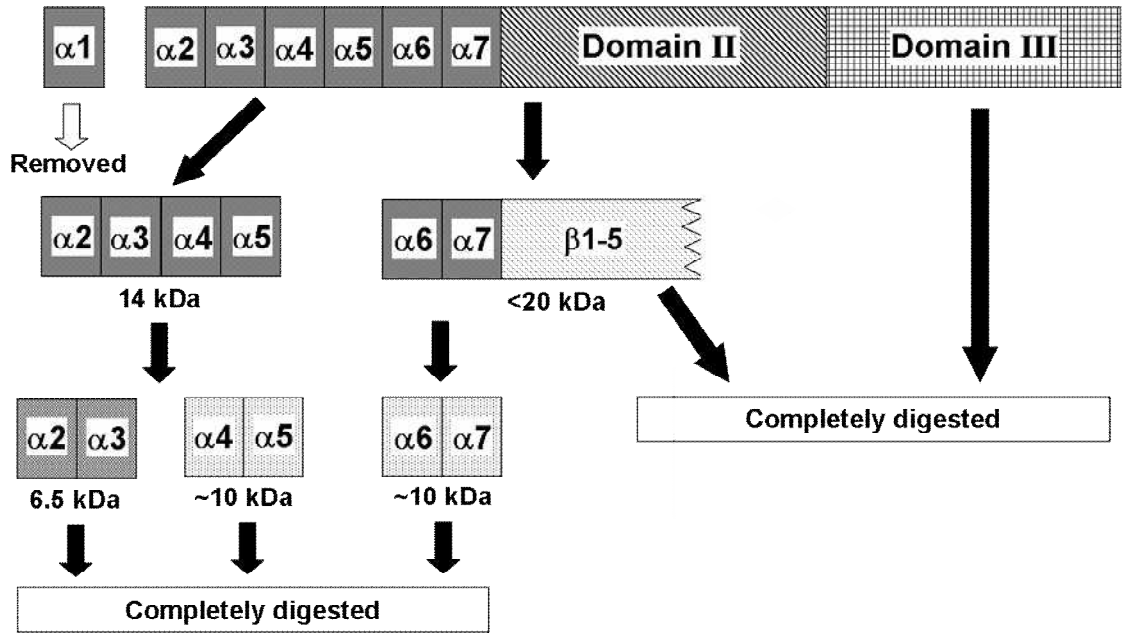

Fig.15. Supposed Fragmentation Pronase digestion manner of free Cry1Ac. α-1 helix eliminated Cry1Ac generated the stretch from α-2 to α-4 helix (14 kDa) and the fragment from α-6 helix to β1-5 sheets (<20 kDa) by the digestion. Furthermore, the 14 kDa fragment was divided into α-2,3 helices (6.5 kDa) and α--4.5 helices (~10 kDa), and the <20 kDa fragment was digested gradually from C-terminal, producing α-6,7 helices (~10 kDa). On the other hand, domain II and III were digested quickly in comparison with domain I. Finally, all of the fragments were digested completely.

1.5.4. Digestion of BBMV-bound Cry1Ac with Pronase

The result of Pronase digestion between BBMV-bound Cry1Aa and Cry1Ac displayed both difference and commonality. The most different point was the endurance against protease. Almost intact Cry1Ac, a 53 kDa fragment, was detected with 2 mg/mL treatment (Fig. 11B and C, lane 2-6), but that was not detected on Cry1Aa (Fig. 9, all panels). Moreover, digestibility of Cry1Ac and the fragments showed no relativity to Pronase concentration from 1 to 2 mg/mL (Fig. 11, all panels). It was clear that BBMV-bound Cry1Ac is fragmented on restricted point only.

Several digests corresponding to fragments generated by BBMV-bound Cry1Aa digestion were observed on also Cry1Ac. Fragment of <6.5 kDa was detected with anti α-2,3 antiserum, and 26-31 kDa fragments were recognized by anti α-4,5 and α-6,7 antisera (Fig. 11A, B and C, lane 2-6); based on the molecular weight, a <6.5 kDa fragment may accord with a 7.5 kDa fragment produced by BBMV-bound Cry1Aa digestion, and 26-31 kDa fragments might be corresponding to 30-35 kDa fragments generated from one (Fig. 9B and C, lane 2-5). A 15 kDa peptide as dimeric α-4,5 helices, however, was not detected with anti α-4,5 antiserum on BBMV-bound Cry1Ac digestion. These results mean that domain I of BBMV-bound Cry1Ac may be fragmented at similar point of Cry1Aa but it does not oligomerize on *B. mori* BBM. As mentioned above, a 53 kDa fragment was recognized by anti α-4,5 and α-6,7 antisera and the fragment existed with 26-31 kDa fragments at the same time (Fig. 11B and C, lane 2-6). It is supposed that BBMV-bound Cry1Ac was fragmented through several complex manners.

On the other hand, anti β-6-11 antiserum detected a 24 kDa fragment (Fig. 11E, lane 2-6), but the fragment may not be equivalent to a 30 kDa fragment on BBMV-bound Cry1Aa digestion because the fragment was not detected by anti domain III antiserum. Only a 6.5 kDa fragment was detected by anti domain III antiserum (Fig. 11F, lane 2-6), proposing domain III conformation on the *B. mori* BBM should be different between Cry1Aa and Cry1Ac. Indeed, homology of domain III on the toxins is only ~50%, therefore, function and conformation of the domain may differ strikingly from each other. Moreover, common 6.5 kDa fragment was detected by anti β-6-11 and anti

domain III antisera (Fig. 11E and F, lane 2-6). This fragment may range from C-terminal end of β-11 sheet to N-terminal end of domain III.

Supposed diagram of BBMV-bound Cry1Ac digestion is exhibited on Fig. 16. Fragmentation flow of BBMV-bound Cry1Ac may be more complex than that of Cry1Aa. Therefore, only the range of each fragment is shown here. Many fragments were produced by Pronase digestion of BBMV-bound Cry1Ac, and all of them were not digested from beginning to end. First, α-1 helix eliminated Cry1Ac is trimmed off α-2,3 helices (<6.5 kDa). Derived from the eliminated Cry1Ac, the stretch from α-4 helix to a part of domain III (53 kDa), the fragment from α-4 helix to a part of β-1-5 sheets (26-31 kDa) and the domain II with N-terminal region of domain III (24 kDa) are generated respectively. In addition to these, the snip including C-terminal end of β-11 sheet and N-terminal end of domain III (6.5 kDa) is produced from some of the parental Cry1Ac fragment. All of these fragments remains in the BBMV although vigorous protease digestion.

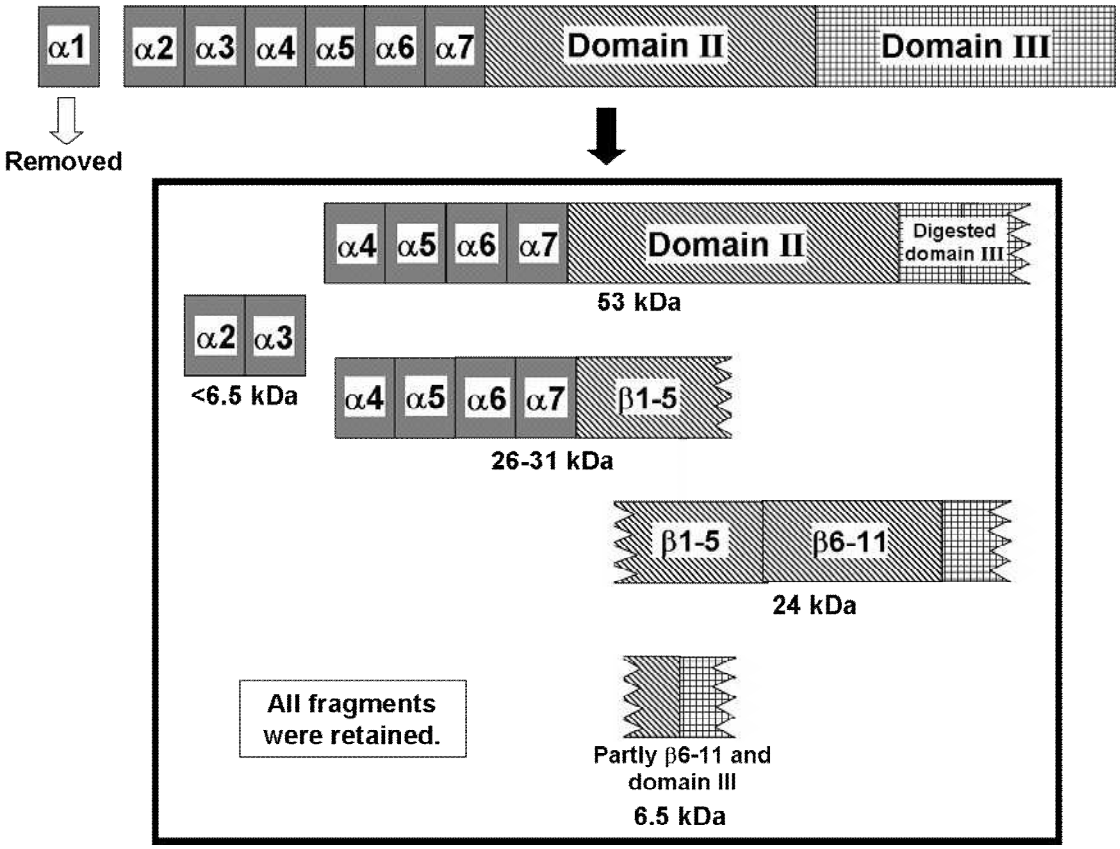

Fig. 16 Tentative fragmentation pattern of BBMV bound Cry1Ac on the result of Pronase treatment. Fragmentation flow of BBMV-bound Cry1Ac was more complex than that of Cry1Aa. Therefore, only range of each fragment is shown here. Five individual fragments were generated by BBMV-bound Cry1Ac digestion, α-2,3 helices (<6.5 kDa), the stretch from α-4 helix to a part of domain III (53 kDa), the fragment from α-4 helix to a part of β-1-5 sheets (26-31 kDa), domain II with N-terminal region of domain III (24 kDa) and the snip including C-terminal end of β-11 sheet and N-terminal end of domain III (6.5 kDa). All of these fragments remained in BBMV without further digestion although vigorous Pronase treatment.

1.5.5. Oligomerization assay of Cry1Aa and Cry1Ac

Oligomerization assay revealed that Cry1Aa and Cry1Ac varied entirely on oligomerization activity. Cry1Aa tetramerized on the BBMV and the tetramer was distributed to both 1% (v/v) Triton X-100 solubilized fraction and insolubilized fraction (Fig. 12A, Sol. and Insol., lane 2). But Cry1Aa did not require necessarily the BBMV to oligomerize since Cry1Aa tetramer was also detected without BBMV (Fig. 12A, Without BBMV, lane 2), It means that Cry1Aa tetramer should be formed before interaction with BBMV and bind directly to BBMV. The tetramer were dissociated by boiling at 95 °C with SDS-PAGE buffer (Fig. 12A, lane 1), suggesting the tetramerization may be caused by hydrophobic interaction but not disulfide bond because SDS-PAGE sample buffer contained 2-mercaptoethanol as strong reducer. Additionally, monomeric Cry1Aa oriented into only insolubilized fraction on 60 °C boiling but the amount was more than tetrameric one (Fig. 12A, Insol., lane 2). A large amount of Cry1Aa monomer might achieve pore formation on the BBM by itself. In fact, Gómez and her colleagues report that monomeric Cry1Aa had somewhat pore forming activity (Gómez et al., 2002b).

In contrast, Cry1Ac did not oligomerize in all cases (Fig. 12B). Moreover, binding amount especially on the insolubilized fraction was remarkably less than Cry1Aa (Fig. 12B, Insol.). These indicate that Cry1Ac forms no oligomer and interacts hardly with the protein or/and the lipid on the insolubilized fraction; i.e. lipid raft which is hydrophobic microdomain containing a large amount of cholesterol, glycolipid and GPI anchored protein such as APN on the plasma membrane (Sato, 2001). Furthermore, partly digested Cry1Ac (~56 kDa) was detected in case of the reaction with BBMV (Fig. 12B, Sol. and Insol.), but the same fragment was not detected in case of Cry1Aa. In Pronase digestion assay of BBMV-bound Cry1Ac, a 53 kDa fragment was detected (Fig. 11B and C, lane 2-6). Based on the molecular weight, perhaps, this 53 kDa fragment and the former ~56 kDa fragment are the identical to each other, indicating BBMV-bound Cry1Ac containing not only ultra-high protease resistance region but also digestible hot spot(s). Partial digestion may deprive Cry1Ac of pore formation ability.

1.5.6. Theory for membrane insertion and pore forming model of Cry1Aa

I tentatively constructed the theory for the membrane insertion and pore forming model of Cry1Aa on the basis of the results obtained by Pronase digestion and oligomerization assays (ref. Fig. 9, 12 and 14). As described above, membrane insertion and pore formation by Cry1Aa may occur independently in the case of the monomer and tetramer toxin. Molecular conformation especially in tertiary and quaternary structure of the toxin locating on the BBM must dramatically differ between monomer and tetramer from each other. Hypothesized models of the membrane insertion and pore formation of Cry1Aa are summarized in Fig. 17.

Monomeric Cry1Aa's model is shown in Fig. 17 (A). The model was named "Buried Dragon model" after the shape of the dragon resting underneath the ground by the author. Monomer of BBMV-bound Cry1Aa has three digestible sites, i.e., loop between α-1 helix and α-2 helix, loop between α-3 helix and α-4 helix, and β-1-5 sheets. This matches with the result that α-2,3 helices and 30-35 kDa fragments including α-4-7 helices were detected simultaneously (Fig. 9A, B and C), and β-1-5 sheets was digested rapidly (Fig. 9D). Thus, these loop structures and β-1-5 sheets may be exposed on the BBM surface. Most importantly, pore forming region of Cry toxin is supposed to be α-2-7 helices in our model. Generally it has been believed that the region involved in the membrane insertion and pore formation in Cry1A toxins is α-4,5 helices (Gazit and Shai, 1995). However, monomeric Cry1Aa must not be able to form a pore with the insertion of single α-4,5 helices because the helices are too small to form and/or keep pore. Generally the size of region inserted into the plasma membrane should be at least ~25 kDa to transverse the membrane structure (Murata et al., 2000). If α-2-7 helices that is constructed of six α-helices penetrate into the BBM, it may be possible to transverse and form a pore even single Cry1Aa monomer.

On the other hand, β-6-11 sheets and domain III may also be buried in the membrane, but these regions may only relate with receptor binding or molecular stability. This is, however, based on a prevailing view, thus more precise investigation is absolutely necessary. Indeed, β-6-11 sheets and domain III also showed protease resistance equivalent to that of domain I (Fig. 9E and F). For explanation of this, domain II and III

must be thought to interact directly with BBM as well as domain I did. Natural physicochemical reason, domain II and III which are constructed of common? antiparallel β-sheets and β-sandwich should not form a pore (P. Boonserm et al., 2005). Perhaps, β-6-11 sheets and domain III are buried, not penetrate, into the BBM and must influence to pore formation via the interaction with the domain I penetrated into the membrane. Recently, it was shown in mosquito larvae that Cry4Aa domain III and the α-7 helix interacted with *Aedes aegypti* midgut (T.K. Boonserm, et al., 2005).

In addition, α-3 helix and α-7 helix were also suggested to be important for pore formation activity of Cry1A toxin in site directed mutagenesis experiments (Vachon et al., 2002; Alcantara et al., 2001). It indicates that numerous parts of domain I and domain III have crucial role(s) on pore formation. The most important idea of the Buried Dragon model is that almost whole molecule of Cry1Aa is buried or penetrates into the BBM. This theory is so innovative that various investigators might say that they don't agree since this model seemed to neglect all past data obtained in molecular biology. However, several reports support this idea that the whole Cry toxin inserts into the membrane (Aronson and Shai, 2001). One of the most important evidences for the "whole Cry toxin insertion" was offered from the pioneer scientist in this field and is that *M. sexta* BBMV-bound Cry1Ac had protease-K resistance since the toxin was protected by the membrane (Aronson et al., 1999).

Counterpart of the single molecule model, oligomeric molecule model is shown in Fig. 17 (B). In this theory, only α-4,5 helices of tetrameric Cry1Aa was suggested to be inserted into the BBM and other parts may be exposed on the membrane surface, because the fragment thought to be originated from tetrameric Cry1Aa was detected as only the 15 kDa peptide which was analogized as α-4,5 helices dimer (Fig. 9B, lane 2-6). Tetramer of α-4,5 helices is composed of eight α-helices and molecular size is ~25 kDa. These molecular size and number of the helices may be enough to form one pore. However, I have to admit that this model connotes two contradictions: First, I presumed that tetrameric Cry1Aa form a pore through tetrameric α-4,5 helices, but actually, the fragment detected by anti α-4,5 antiserum must be a dimer, inferred from the molecular weight. An appropriate idea which explains this paradox is that tetrameric α-4,5 helices

was degraded to the dimer by Pronase digestion or denaturation during SDS-PAGE sample preparation. In fact, oligomerized Cry1Aa on the BBM was only tetramer (Fig. 12A, lane 2). Secondary, if only α-4,5 helices inserts into the BBM, the pore may not maintain due to uninserted ~60 kDa remnant, extra α-helices with domain II and III, because these obstacle regions must cause steric hindrance of Cry1Aa. One of the presumed solutions for the discrepancy is that uninserted region is digested by the protease secreted from insect midgut. As a result, membrane insertion region should avoid steric hindrance.

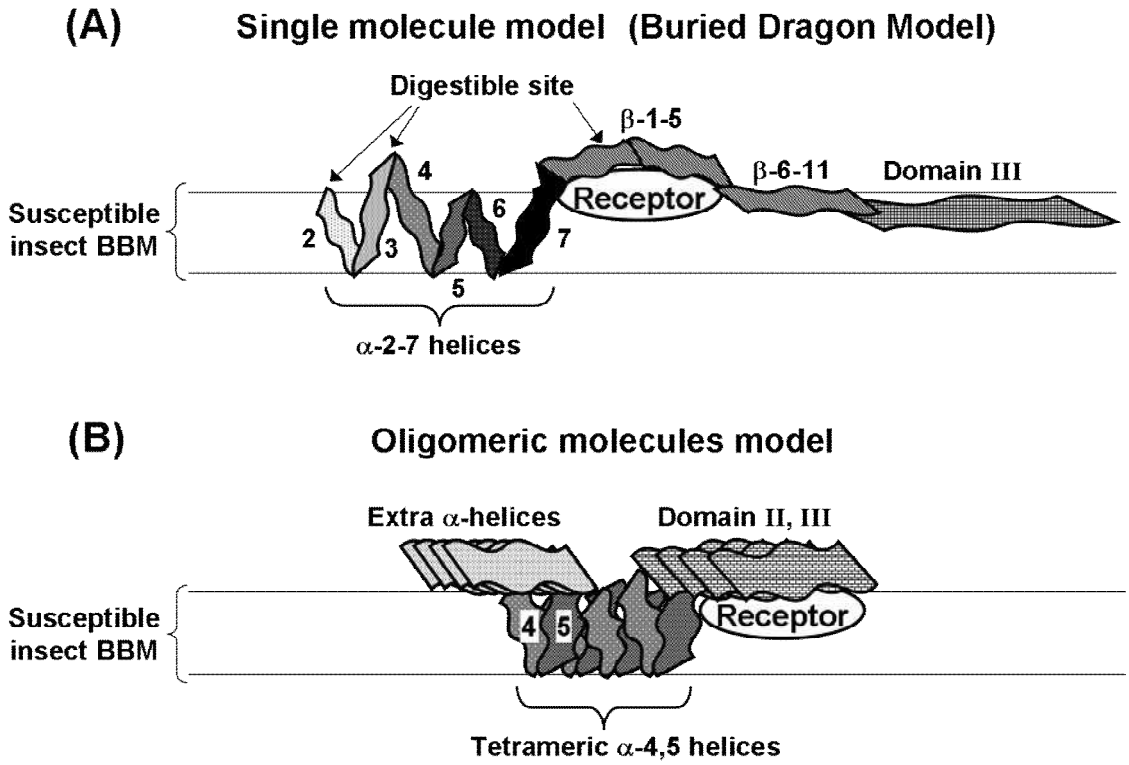

Fig. 17 Plausible membrane insertion and pore forming model of Cry1Aa based on the result of Pronase digestion and oligomerization assay of BBMV-bound Cry1Aa. Cry1Aa should insert into the membrane and form a pore on the two conformations; one is monomer, another is tetramer. (A) In case of the single-molecule Cry1Aa, membrane insertion and pore forming regions must be the stretch of α-2 to α-7 helices. Also β-6-11 sheets and domain III were hardly digested, indicating that these regions strongly interact with the lipid membrane, namely, it may be buried into the BBM. α-1 helix, loop between α-3 and α-4 helix and β-1-5 sheets were thought to be exposed on the membrane surface based on the digestibility of these site. (B) Tetrameric α-4,5 helices are suggested to be pore forming region on oligomeric Cry1Aa. Extra α-helices and domain II and III may be on the membrane surface and digested by midgut protease to avoid steric hindrance of Cry1Aa.

1.5.7. Difference of insecticidal specificity between Cry1Aa and Cry1Ac

Based on the result of Pronase digestion assay, I hypothesize the insecticidal specificity mechanism of Cry1Aa and Cry1Ac against *B. mori*. As stated on **1.2. Introduction**, both the toxins bind with *B. mori* BBMV proteins under native and denatured conditions (Shitomi et al., 2006), suggesting the difference between Cry1Aa and Cry1Ac is in localizing mainly membrane insertion step rather than receptor binding step, in other words, high-order structure of the toxins on the BBM is important crucially for insecticidal specificity. Actually, the digestibility as the index of molecular conformation differed widely between Cry1Aa and Cry1Ac (ref. Fig. 9 and 11). Unexpectedly, Cry1Ac was digested hardly compared to Cry1Aa. It is supposed that Cry1Ac may be able to insert into *B. mori* BBM despite the toxin exhibits no insecticidality toward *B. mori* or it might not be forming a pore on the BBM.

I deliberate the phenomena that Cry1Ac inserts into *B. mori* BBM but the insertion is not led to pore formation and the epithelial cell death. My idea is visualized on Fig. 18. Cry1Ac may bind with some receptor(s) and the whole molecule except domain III into the BBM because almost region of Cry1Ac was detected as <6.5 kDa, 26-31 kDa and 24 kDa fragments, furthermore, a 53 kDa fragment corresponding to nearly full-length Cry1Ac was also protected by the membrane (See *1.5.4. Digestion of BBMV-bound Cry1Ac with Pronase* and Fig. 11). However, these membrane inserted regions do not promote to form a pore. Incidentally, C-terminal region of domain III was digested completely (Fig. 11F). Domain III interacts with GalNAc residue of sugar side chain attached to lipid or protein through its GalNAc binding site (Knight et al., 1994), therefore, the domain should be anchored by sugar side chain on the BBM surface and it may be exposed on the BBM surface. Suggestively, it is revealed that Cry1Ac does not form tetramer on *B. mori* BBM by the direct and indirect evidence; the former is that Cry1Ac occurred oligomerization neither with *B. mori* BBM nor without one (Fig. 12B), and the latter is that a 15 kDa fragment according to dimeric α-4,5 helices was not detected on the digestion of BBMV-bound Cry1Ac (Fig. 11B). Oligomer formation must be impossible to *B. mori* BBMV-bound Cry1Ac, and it should be disadvantage of Cry1Ac on the pore forming since oligomer Cry1A toxin has >10 times higher pore

forming activity in comparison with that of monomer (Gómez et al., 2002b).

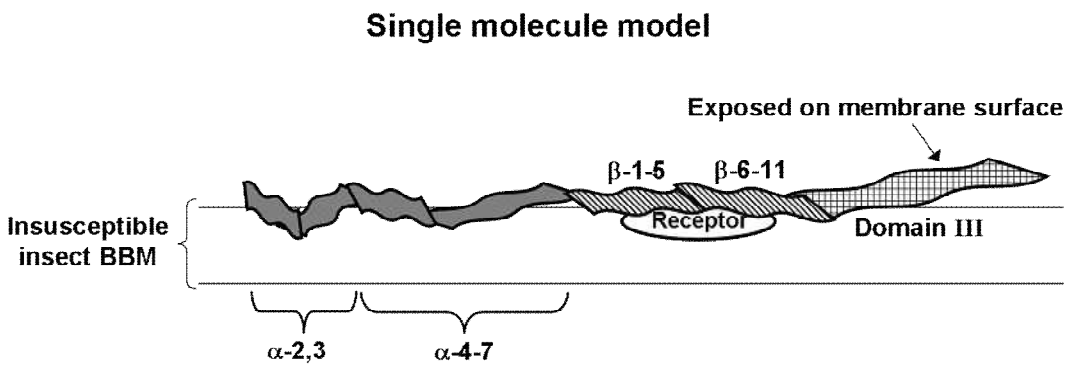

Fig. 18 Membrane insertion model of Cry1Ac suggested from Pronase digestion and oligomerization assay of BBMV-bound Cry1Ac. Almost whole Cry1Ac may be buried into *B. mori* BBM but it does not lead to pore formation differs from Cry1Aa. Only C-terminal half of domain III may be exposed on the membrane surface.

I predict presumed membrane interaction model of Cry1Ac. It may quietly differ from Cry1Aa (Fig. 17 vs. Fig. 18). Almost part of Cry1Ac may interact with and be buried into *B. mori* BBM but it has never penetrated into the membrane. Moreover, several reports indicated the other diversity between Cry1Aa and Cry1Ac on the toxicity against *B. mori*. For example, peritrophic membrane permeability of Cry1Aa and Cry1Ac was different from each other. Cry1Aa passed through peritrophic membrane constantly, but Cry1Ac was trapped in the membrane for about 2 h (Hayakawa et al., 2004). Trapped Cry1Ac may be digested partly by the midgut juice and should be lost the pore forming or insecticidal activity. Recently, other indicative reports were published. The report advocated “Decoy-receptor binding hypothesis” that Cry1Ac would be trapped by not only peritrophic membrane also midgut protein such as 96 kDa APN (Shitomi et al., 2006) and P252 (Hossain et al., 2004). Pseudo-receptor may bind initiatively with Cry1Ac, but the binding does not lead to form a pore.

Binding amount of monomeric Cry1Aa was much more than that of Cry1Ac, especially on the Triton X-100 insolubilized fraction or raft fraction (Fig. 12A and B, Insol.). Low interactivity of Cry1Ac with lipid raft may be one of the reasons that Cry1Ac does not display insecticidality against *B. mori* because several important receptors for Cry1Ac such as APN locate on raft fraction of the BBM (Zhuang et al., 2002; Bravo et al., 2004). Thus, many factors must relate with the insecticidal activity between Cry1Aa and Cry1Ac against *B. mori*.

Chapter 2

Comparative study of glycosyltransferases activity in between Cry1Ac susceptible and resistance *Plutella xylostella* midgut

2.1. Abstract

Cry toxin is the insecticidal protein produced by *Bacillus thuringiensis*, Gram-positive soil bacteria, and the toxicity is performed through pore formation on the brush border membranes (BBM) of midgut epithelial cells. Galactose and GalNAc transferase activity were measured and compared between midgut of Cry1Ac susceptible *Plutella xylostella* (PXS) and resistant one (PXR) to reveal the resistant mechanism. Galactose was incorporated into both chloroform/methanol solubilized and insolubilized fraction, but GalNAc was taken in almost insolubilized fraction. It is thought that galactose residue may be existed on both glycolipid and glycoprotein, but GalNAc may be incorporated into glycoprotein predominantly. Interestingly, galactosyltransferase activity was almost same on both of strains, but GalNAc transferase activity was 1.5-2 times higher on PXS compared to PXR. Based on the result of thin layer chromatography, galactosylated glycolipids were detected mainly as mono- to tetrasaccharylceramide, and the glycolipid including GalNAc residue was principally tetrasaccharylceramide. Galactose may incorporate into neogala-series glycolipid and GalNAc would be taken into arthro-series glycolipid. Amount of the tetrasaccharylceramide incorporating GalNAc was much higher on PXS compared with PXR. Tetrasaccharylceramide amount must influent synthesis of the saccharylceramides which is attached $\geqq$pentasaccharide because tetrasaccharylceramide is precursor of one. Thus, the diversity of glycolipid component between PXS and PXR may affect formation of the membrane microdomain such as “raft” and membrane interactivity of Cry1Ac. It must be one of the crucial reasons of Cry1Ac resistance of PXR.

2.2. Introduction

As mentioned on **General introduction**, *B. thuringiensis* and Cry toxin gene have been widely used for biopesticide and foreign gene in transgenic crops. However, one of the most serious problems is that the resistant strain insect against Cry toxin has appeared through continuous utilization of the biopesticide as well as chemical pesticide on the field (Wirth et al., 1998; Sayyed et al., 2000; Zhao et al., 2000; Griffitts and Aroian, 2005). General resistant mechanism is not cleared completely, but it was clarified partially in some insects. For instance, the receptor protein reducing was reported as the resistance mechanism in *H. armigera* (Van Rie et al., 1990), and the binding ability of BBMV protein toward Cry1A toxins differed between susceptible and resistant strain on *Pectinophora gossypiella*, *H. armigera* and *O. nubilalis* (González-Cabrera et al., 2003; Luo et al., 2006; Siqueira et al., 2006). On the other hand, in *Plutella xylostella*, it was demonstrated that the binding ability of BBMV prepared form resistant strain to Cry1Ac was much lower than that of susceptible strain (Tabashnik et al., 1994b), and Cry1Ac resistance strain of *S. exigua* lacked one of four APN genes (Herrero et al., 2005). But there is also the report that the binding ability did not relate with the resistant mechanism on *Plutella xylostella* (Kato et al., 2006). Thus, the inclusive resistance mechanism is unclarified at present.

Previously, our laboratory reported that total amount of neutral glycolipid extracted from resistant *P. xylostella* midgut was half as that of susceptible strain (Kumaraswami et al., 2001), moreover, the diversity was significant on glycolipids that were attached to 4< sugar residues. Recently, Griffitts and his collaborators demonstrated the glycolipid obtained from Cry5B susceptible *Caenorhabditis elegans* bound with toxin but resistant one did not, in addition, resistant strain mutated several glycosyltransferase genes (Griffitts et al., 2001, 2003 and 2005). And then, Cry1Ac has *N*-acetylgalactosamine (GalNAc) binding site and recognizes GalNAc residue of sugar side chain added to receptor protein such as APN (Knight et al., 1994; Carroll et al., 1997; Cooper et al., 1998). Furthermore, Cry1A resistant *H. armigera* altered in BBM protein glycosylation pattern compared to susceptible strain, and the proteins decreased binding ability to Cry1A toxins (Jurat-Fuentes, et al., 2002). These reports strongly represent that BBM

glycolipids and glycoproteins relate with Cry toxin tolerance.

P. xylostella is one of the serious insect pests against brassicae crops and expresses high Cry1Ac resistance on the field and laboratory (Ferre et al., 1991; Tabashnik, 1994a; González-Cabrera et al., 2001; Baxter et al., 2005). Our laboratory has investigated Cry1Ac resistance mechanism of *P. xylostella*. I noted particularly the diversity of glycolipids between Cry1Ac susceptible *P. xylostella* (PXS) and resistant one (PXR) (Kumaraswami et al., 2001), and expected that PXR extinguishes glycosyltransferase gene(s) same as *C. elegans*'s case. In fact, it was reported that *M. sexta* neutral glycolipid associated with APN interacted with Cry1Ac (Sangadala et al., 2001). Therefore, I measured and compared activity of two glycosyltransferase, galactosyltransferase (GalT) and *N*-acetylgalactosaminyltransferase (GalNAcT), on PXS and PXR. It is rational that measuring GalT and GalNAcT activity because GalNAc residue interacts with Cry1Ac, and a 47 kDa protein (P47) lacked on PXR midgut was identified as galactosidase by MALDI-TOF/MAS analysis (Mahmood et al., unpublished data). P47 may invest also galactosyltransferase activity because depolymerization enzymes such as DNase are often able to catalyze reverse reaction or polymerization reaction. Moreover, galactose and GalNAc is added restrictively behind 3rd sugar residue from reducing terminus in arthropod glycolipid (Wiegandt, 1992); described above, diversity of the glycolipid amount was significant on >tetrasaccharylceramide.

Nowadays, several countermeasures against insect pests inherited Cry toxin resistance is contrived. One of the good strategies is to utilize simultaneously two or more Cry toxins for pesticide or transgene into transgenic crop (Zhao et al., 2003). To clarify the resistance mechanism will benefit to grope the combination of various Cry toxin that is effective in the prevention against birth of Cry toxin resistance strain.

2.3. Material and method

2.3.1. Insect

Susceptible and resistant strains of *P. xylostella* that were isolated from Kishiwada, Osaka, Japan were contributed from Dr. Takeshi Maruyama, and they were fed with artificial diet that was made mainly of powdered soybean and wheat germ. PXR has ~100,000 times Cry1Ac resistance compare to PXS (Maruyama et al., 1999).

2.3.2. Activity measurement of GalT or GalNAcT on P. xylostella midgut

Midguts were isolated from 4th instar larvae of PXS or PXR on ice and stored in MET buffer (50mM Tris-HCl, 300 mM mannitol, 5mM EGTA, 1 mM PMSF, pH 7.4). About 300 midguts were homogenized in HEPES-NaOH, pH 7.4 containing Protease Inhibitor Cocktail for General Use (1x) (Sigma-Aldrich), 20 μM CDP-choline, 2 mM ATP, 0.2 mM BAL, 20 μM galactonolactone, and protein concentration of the homogenate was adjusted to 10 mg/mL. One μL of Uridine diphosphate galactose [galactose-6-^{3}H] (37 kBq/μL, 740 Bq/pmol; American Radiolabeled Chemicals, St. Louis, MO, USA) or 2 μL of Uridine diphosphate *N*-acetyl-D-galactosamine[galactosamine-6-^{3}H(N)] (18.5 kBq/μL, 740 Bq/pmol; American Radiolabeled Chemicals) was mixed with 99 μl homogenate and reacted for 3h at 30 °C. Final concentration of labeled sugar-nucleotide was 50 nM, and the total amount of each labeled sugar nucleotide was 50 pmol. After reaction, the midgut homogenate was centrifuged at 500 × *g* for 10 min at 4 °C. The pellet was recovered as nucleus and cell debris fraction (Nuc./CellDeb.), and the supernatant was re-centrifuged at 20,000 × *g* for 10 min at 4 °C. The pellet was recovered as mitochondria and lysosome fraction (Mito./Lyso.) and the supernatant as microsome and cytosol fraction (Micro./Cyto.). These fractions were extracted with 1 mL of chloroform/methanol/100 mM acetic acid (1/1/0.9) for 30 min at 180 rpm to form organic, middle and water phase by centrifugation of 20,000 × *g* for 5 min at 25 °C (Fig. 19). The water and middle phase was mixed with 1/9 volume of 100% (w/v) trichloroacetic acid (TCA) and placed on ice for 1 h. The sediment was recovered through centrifugation at 20,000 × *g* for 5 min at 4 °C. TCA precipitate was washed twice with 90% (v/v) acetone. On the other hand, the unreacted labeled sugar-nucleotide in organic phase was removed by two-phase distribution with chloroform saturated with 50% (v/v) methanol. Finally, organic solvent of all samples were evaporated with centrifugal concentrator. Each experiment was independently done four times.

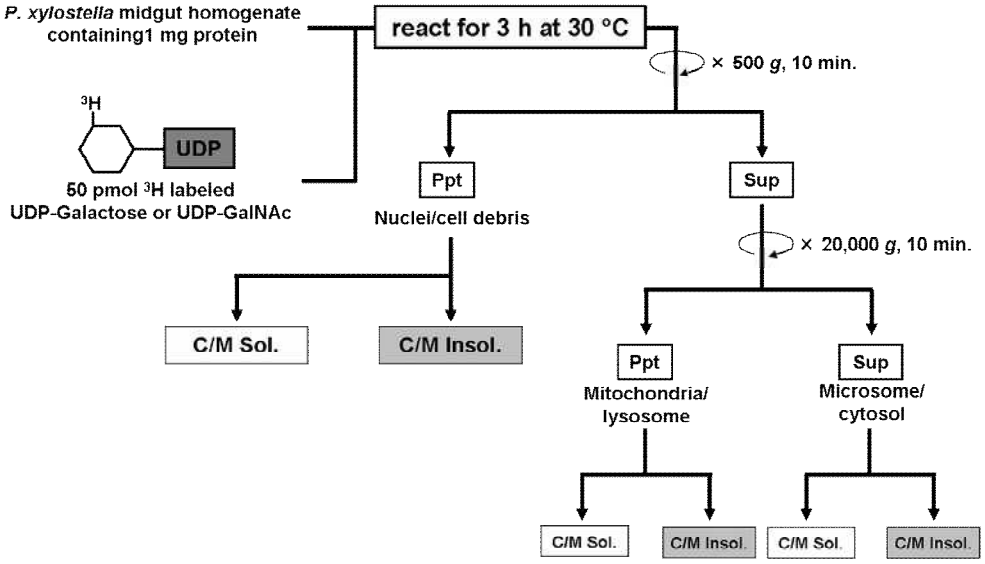

Fig. 19 Methodology of GalT and GalNAcT activity measurement. See *2.3.2. Activity measurement of GalT and GalNAcT on P. xylostella* midgut in detail.

2.3.3. Activity measurement of GalT or GalNAcT with $MnCl_2$

Activity measurement of both enzymes with $MnCl_2$ was performed to examine the effect of Mn^{2+} on *P. xylostella* glycosyltransferase activity. It was achieved basically by the method shown in *2.3.2. Activity measurement of GalT and GalNAcT in P. xylostella midgut* was done with addition of 10mM $MnCl_2$ to the reaction buffer. However, cell fractionation was not done as $MnCl_2$ induces the aggregation of midgut homogenate. Each experiment was independently done four times.

2.3.4. Liquid scintillation counting

Chloroform-methanol solubilized fractions (C/M Sol.) were dissolved directly in 5 mL OCS Scintillation Cocktail (GE Healthcare Bio-Sciences). On the other hand, chloroform-methanol insolubilized fraction (C/M Insol.) were solubilized with NCS Tissue Solublizer (GE Healthcare Bio-Sciences) for 1 h at 30 °C and then mixed with 5 mL OCS. All samples were incubated at room temperature for 2h to quench chemiluminescence and measured its radioactivity by liquid scintillation counter for 5 min at 25 °C. The counting efficiency was determined by external standard method.

2.3.5. TLC analysis of the labeled sugar incorporated in glycolipid

C/M Sol. isolation from PXS or PXR midgut were achieved by the method as in *2.3.3. Activity measurement of GalT or GalNAcT with $MnCl_2$*. Each C/M Sol. was developed and separated by thin layer chromatography (TLC) plate (25 HPTLC-Plates 10 × 10 cm Silica gel 60; Merck, Darmstadt, Germany) with chloroform/methanol/DDW (65/35/8) as the development solvent and Neutral Glycolipid for TLC (Iso Sep AB, Tullinge, Sweden) were used as the molecular standard for glycolipid. Separated glycolipids was detected by BAS-5000 (FUJIFILM, Kanagawa, Japan), and the glycolipid standard was visualized with orcinol/sulfuric acid reagent.

2.4. Result

2.4.1. Activity measurement of GalT or GalNAcT on P. xylostella midgut

Galactose and GalNAc were incorporated into both PXS and PXR midgut homogenate, but these sugars was observed to differ widely in the C/M Sol. to C/M Insol. distribution ratio, and also the total incorporated amount of both sugars between PXS and PXR was observed to be different.

Galactose intake rate of each cell fraction in the C/M Sol. was ~30-40% into Nuc./CellDeb., ~15-20% into Mito./Lyso. and ~45-50% into Micro./Cyto. In the case of C/M Insol., the rate was ~50-55% into Nuc./CellDeb., ~15-20% into Mito./Lyso. and ~25-30% into Micro./Cyto. However, no significant difference was confirmed in their incorporated amount between PXS and PXR except for that in Nuc./CellDeb (PXS was 1.4 times as PXR on the fraction). On the other hand, ratio of C/M Sol. to C/M Insol was about 1 to 3 on the whole (Fig. 20, Table 2).

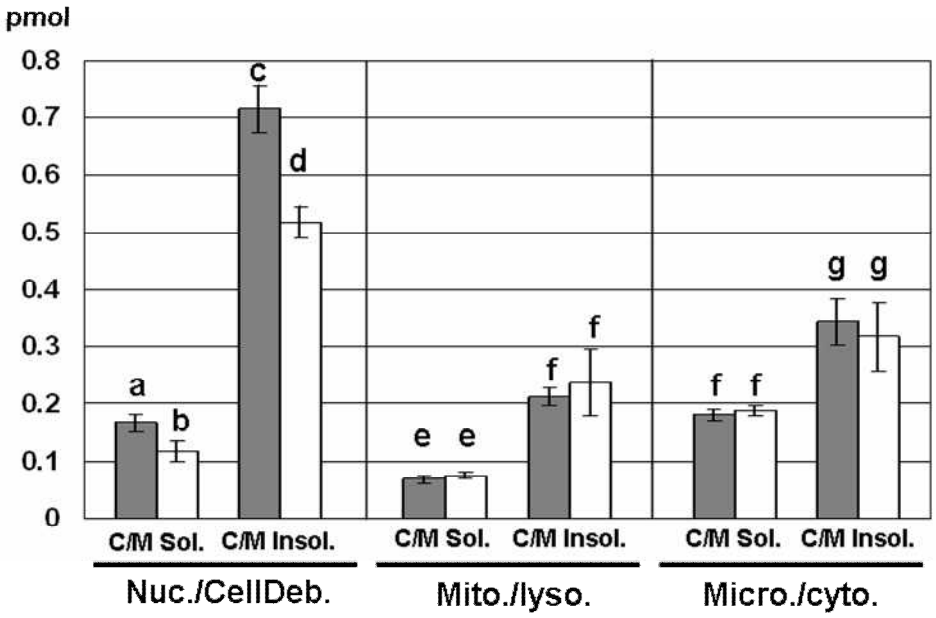

Fig. 20 Galactose incorporation to Cry1Ac susceptible and resistant *P. xylostella* midgut tissue. One µL of ^{3}H labeled UDP-galactose (50 pmol, 37 kBq) was mixed with midgut homogenate containing 1 mg protein and reacted for 3 h at 30 °C. After the reaction, each cell component fraction, nucleus/cell debris fraction, mitochondria/lysosome fraction and microsome/cytosol fraction, were separated by appropriate centrifugation. Each fraction was extracted with chloroform/methanol/100 mM acetic acid (1/1/0.9) and the extract was separated into organic and water phase through centrifugation. After removal of free labeled UDP-sugar by appropriate method, radioactivity of each sample was measured by liquid scintillation counter. Shown in the left panel is nuclear and cell debris fraction, middle is mitochondria and lysosome fraction and right is microsome cytosol fraction. Vertical axis shows intake amount (pmol). C/M Sol. and C/M Insol. mean chloroform/methanol/100 mM acetic acid (1/1/0.9) solubilized fraction and insolubilized fraction, respectively. Gray bar indicates the result of PXS and white bar is of PXR. Average and standard deviation were calculated from four independent experiments. Significant difference was examined with Student t-test and it was corroborated by different alphabets above each bar ($p<0.05$). The same alphabets imply insignificance.

Table 2 Summary of galactose incorporation into each cell fraction of *P. xylostella* midgut tissue. On each box, upper number is the incorporation amount in pmol, and parenthesized number is the incorporation ratio of total amount in percentage.

	Amount of galactose incorporation (pmol) (Distribution (%))							
	Nuc./CellDeb.		Mito./Lyso.		Micro./Cyto.		Total	
	C/M Sol.	C/M Insol.	C/M Sol.	C/M Insol.	C/M Sol.	C/M Insol.	C/M Sol.	C/M Insol.
PXS	0.17 (41)	0.72 [57]	0.069 (16)	0.21 [16]	0.18 (43)	0.34 [27]	0.42 (100)	1.3 [100]
Ratio of Sol. to Insol.	19	81	25	75	35	65	24	76
PXR	0.12 (31)	0.52 [48]	0.075 (19)	0.24 [22]	0.19 (50)	0.32 [30]	0.39 (100)	1.1 [100]
Ratio of Sol. to Insol.	19	81	24	76	37	63	26	74
PXS/PXR	1.4	1.4	0.92	0.88	0.95	1.1	1.1	1.2

Alternatively, GalNAc was found to be incorporated into almost all C/M Insol. in both the strains and the rate of each cell fraction on the fraction was ~45-50% into Nuc./CellDeb., ~15-20% into Mito./Lyso. and 30-40% into Micro./Cyto. The tendency resembled the galactose incorporation. The difference in the intake amount between PXS and PXR was remarkable when compared to that with galactose intake. Especially, incorporation into Nuc./CellDeb. and Micro./Cyto. on PXS was 1.5 and 2.1 times higher than that of PXR, respectively (Fig. 21, Table 3).

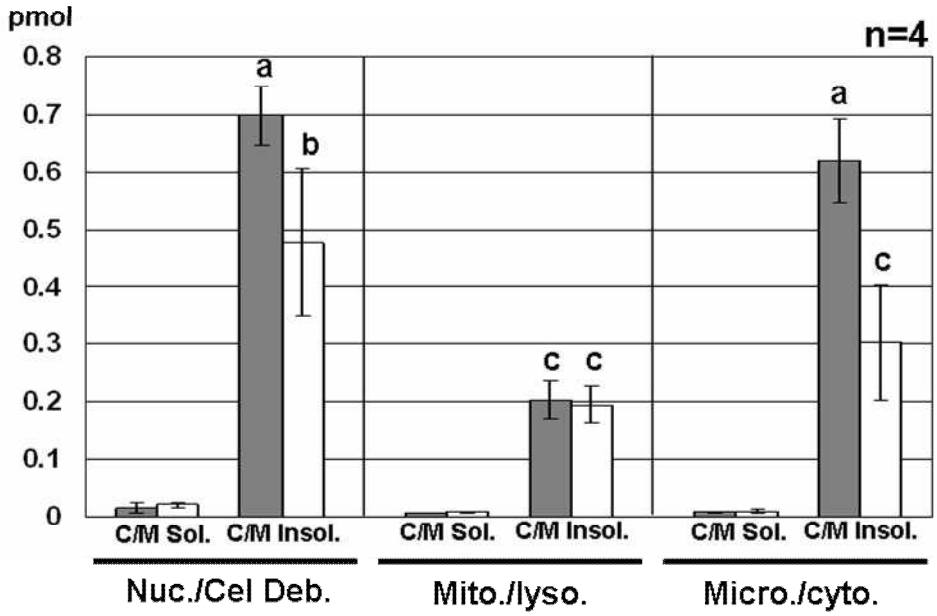

Fig. 21 GalNAc incorporation to Cry1Ac susceptible and resistant *P. xylostella* midgut tissue. Sample preparation and detection method was same as in galactose incorporation experiment except ^{3}H labeled UDP-*N*-acetylgalactosamine (50 pmol, 37 kBq) was used instead of ^{3}H labeled UDP-galactose. Shown in the left is nuclear and cell debris fraction, middle is mitochondria and lysosome fraction and right is microsome cytosol fraction. Vertical axis shows intake amount (pmol). C/M Sol. and C/M Insol. mean chloroform/methanol/100 mM acetic acid (1/1/0.9) solubilized fraction and insolubilized fraction, respectively. Gray bar is the result of PXS and white bar is result of PXR. Significant different test was done same as caption of Fig. 20.

Table 3 Summary of GalNAc incorporation into each cell fraction of *P. xylostella* midgut tissue. On each box, upper number is the incorporation amount in pmol, and parenthesized number is the incorporation ratio of total amount in percentage.

	Amount of GalNAc incorporation (pmol) (Distribution (%))							
	Nuc./CellDeb.		Mito./Lyso.		Micro./Cyto.		Total	
	C/M Sol.	C/M Insol.	C/M Sol.	C/M Insol.	C/M Sol.	C/M Insol.	C/M Sol.	C/M Insol.
PXS	0.015 (54)	0.70 [46]	0.0051 (18)	0.20 [13]	0.0079 (28)	0.62 [41]	0.028 (100)	1.5 [100]
Ratio of Sol. to Insol.	2	98	2	98	1	99	2	98
PXR	0.020 (53)	0.48 [49]	0.0078 (21)	0.19 [20]	0.0097 (26)	0.30 [31]	0.038 (100)	0.97 [100]
Ratio of Sol. to Insol.	4	96	4	96	3	97	4	96
PXS/PXR	0.75	1.5	0.65	1.1	0.81	2.1	0.74	1.5

2.4.2. Activity measurement of GalT or GalNAcT with $MnCl_2$

Activity of GalT and GalNAcT of *P. xylostella* were accelerated by Mn^{2+} (Fig. 22, Table 4). Total GalT activity of PXS and PXR was increased by Mn^{2+} to 1.9 and 1.5 times, respectively. In contrast, total GalNAcT activity was promoted to 4 times against Mn^{2+} free on both of strains.

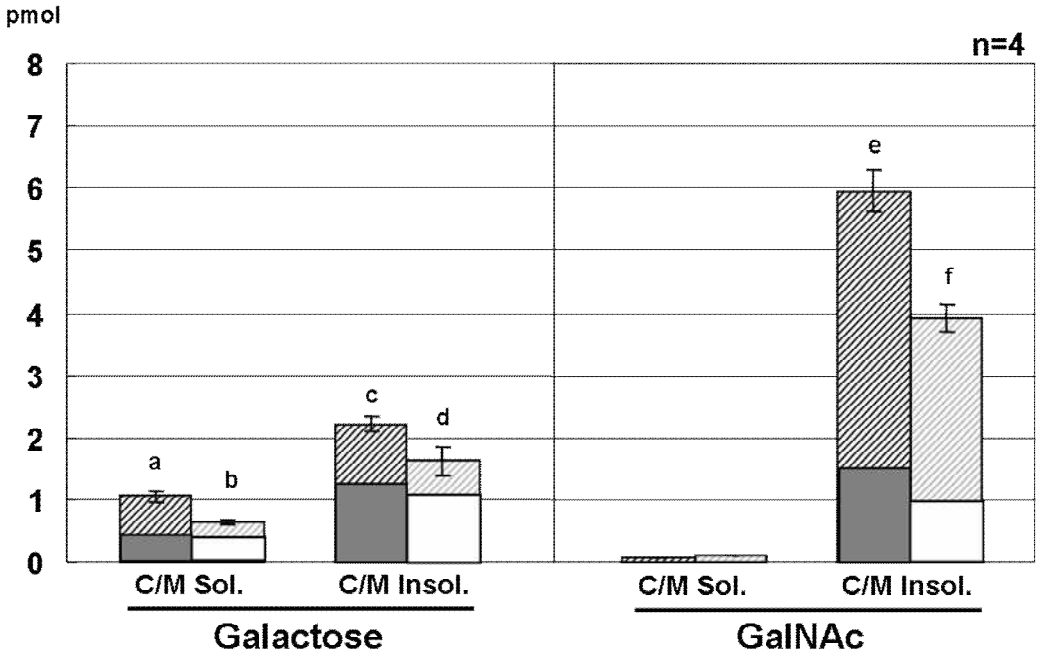

Fig. 22 Galactose and GalNAc incorporation into Cry1Ac susceptible and resistant *P. xylostella* midgut with 10 mM $MnCl_2$. Sample preparation was done as in 2.2.2 Activity measurement of GalT and GalNAcT on *P. xylostella* midgut but cell fractionation was not performed since $MnCl_2$ caused aggregation of the midgut homogenate. Shown in the left is the result of galactose intake and right is result of GalNAc intake. C/M Sol. and C/M Insol. mean chloroform/methanol/100 mM acetic acid (1/1/0.9) solubilized fraction and insolubilized fraction, respectively. Gray bar is the result of PXS and white bar is result of PXR, slashed bar and plain bar indicate incorporation with and without $MnCl_2$ respectively. The result of incorporation without $MnCl_2$ was the summed intake of each cell fraction shown on Fig. 20 and Fig. 21. Significant different test was done same as caption of Fig. 20.

Table 4 Summary of galactose and GalNAc incorporation into whole midgut tissue of *P. xylostella* with or without 10 mM $MnCl_2$. On each box, upper number is the incorporation amount in pmol, and parenthesized number is the incorporation ratio of total amount in percentage.

		Amount of sugar incorporation (pmol) (Ratio of Sol. to Insol.)					
		Galactose			GalNAc		
		C/M Sol.	C/M Insol.	Total	C/M Sol.	C/M Insol.	Total
PXS	(+) Mn^{2+}	1.1 (33)	2.2 (67)	3.3 (100)	0.070 (1)	6.0 (99)	6.1 (100)
	(-) Mn^{2+}	0.42 (24)	1.3 (76)	1.7 (100)	0.028 (2)	1.5 (98)	1.5 (100)
PXR	(+) Mn^{2+}	0.64 (29)	1.6 (71)	2.2 (100)	0.10 (3)	3.9 (97)	4.0 (100)
	(-) Mn^{2+}	0.39 (26)	1.1 (74)	1.5 (100)	0.038 (4)	0.97 (96)	1.0 (100)
PXS/PXR	(+) Mn^{2+}	1.7	1.4	1.5	1.4	1.5	1.5
	(-) Mn^{2+}	1.1	1.2	1.1	0.74	1.6	1.5

2.4.3. TLC analysis of labeled sugar incorporated glycolipid

Various glycolipids incorporating each ^{3}H labeled sugar were detected by TLC analysis (Fig. 23). Five glycolipids incorporating galactose, mono-, di-, tri-, tetra-, > pentasaccharylceramide were detected on both of strains. Tri- and tetrasaccharylceramide were major component and mono- and disaccharylceramide of PXR were slightly less than that of PXS (Fig. 23, Galactose).

On the other hand, tetra- and >pentasaccharylceramide incorporating GalNAc were recognized in both of the strains. Tetrasaccharylceramide amount of PXS was much higher than that PXR (Fig. 23, GalNAc).

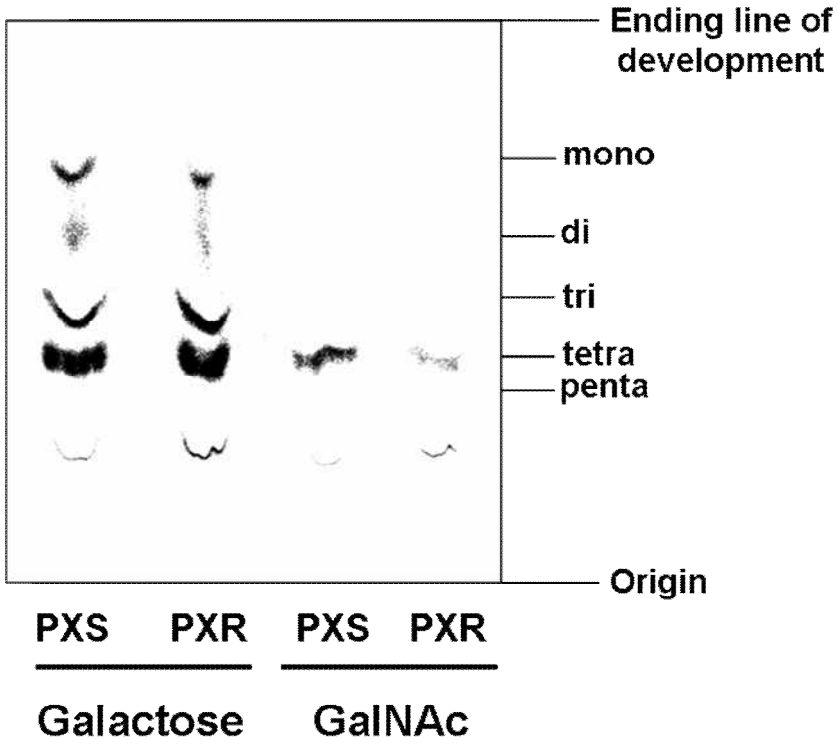

Fig. 23 TLC analysis of glycosylceramide incorporating ^{3}H labeled sugar. Sugar intake reaction was performed with $MnCl_2$. Chloroform/methanol solubilized fraction extracted from whole midgut homogenate without cell fractionation was spotted onto silica gel TLC plate and developed by chloroform/methanol/water (65/30/8). Detection was done by autoradiography. S: susceptible strain; R: resistant strain. Numbers from mono to penta is development point of the standard glycolipid.

2.5. Discussion

2.5.1. Activity of GalT and GalNAcT on P. xylostella midgut

Galactose and GalNAc incorporation assay of PX midgut homogenate had demonstrated interesting results. ^{3}H labeled galactose was incorporated into both of C/M Sol. containing lipids as sugar recipient and C/M Insol. including proteins as one (Fig. 20, Table 2). Incorporation amount ratio of C/M Sol. to C/M Insol. was 1 to 3. This result indicates that galactose incorporation is dominant in glycoprotein rather than glycolipid. The order of intake amount of each cell fraction on the C/M Sol. was Micro./Cyto. > Nuc./CellDeb. > Mito./Lyso., and the order on the C/M Insol. was Nuc./CellDeb. > Micro./Cyto. > Mito./Lyso. Significant comparison of the incorporation amount applies to only Mito./Lyso. and Micro./Cyto. since Nuc./CellDeb. must contain various unfractionated cell components. It is interpreted easily that galactose incorporation amount in Micro./Cyto. was more than in Mito./Lyso. In general, glycosylation occurs in glycosyltransferase-rich organelles like endoplasmic reticulum and golgi apparatus and these cell organelles are included in Micro./Cyto. rather than Mito./Lyso. Incorporation into Mito./Lyso. might be the result of transport of glycoprotein and glycolipid from golgi apparatus, in other words, galactose incorporation may not occur directly in Mito./Lyso. Galactose incorporation ratio of C/M Sol. to C/M Insol. and the rate of each cell fraction had shown almost the same tendency between PXS and PXR, but the amount incorporated itself slightly differed. In Nuc./CellDeb., the incorporation amount on PXS was 1.4 times higher than PXR but the almost no difference was observed incase of other two fractions (0.9-1.1 times). This result suggests that the difference of GalT activity between PXS and PXR may not have a crucial effect on Cry toxin resistant mechanism.

On the other hand, result of the incorporation assay of ^{3}H labeled GalNAc differed considerably from galactose one (Fig. 21, Table 3). GalNAc incorporation was detected virtually in C/M Insol. and not in C/M. Sol. whereas galactose was found to be incorporated into both these fractions. It is thought that GalNAc residue of sugar side chain exists on glycoprotein predominantly. The order of Intake amount of each cell fraction on the C/M Insol. was Nuc./CellDeb. > Micro./Cyto. > Mito./Lyso. This pattern

was same as galactose incorporation, suggesting *N*-acetylgalactosaminylation might occur in Micro./Cyto. as well as galactosylation. Interestingly, GalNAc incorporation amount was different between PXS and PXR. Incorporation amount on PXS was 1.5 and 2 times higher than that of PXR in Nuc./CellDeb. and Micro./Cyto., respectively. This result means that GalNAc residue of PXR midgut glycoprotein is less than PXS one. GalNAc is thought of important sugar to interact with Cry1Ac (Knight et al., 1994), therefore, it may be the evidence that GalNAcT activity relates directly with Cry toxin resistant mechanism.

Generally, glycosyltransferase requires Mn^{2+} for the activity. Mn^{2+} effect, however, was ignored in my experiments due to chelation by 1 mM EDTA contained in Protease Inhibitor Cocktail for General Use (Sigma-Aldrich) that I used. Then, I examined the influence of Mn^{2+} toward GalT and GalNAcT (Fig. 22, Table 4). Both of the enzymes were activated by Mn^{2+} compared to that observed with Mn^{2+} free, the ratio was 1.5-1.9 and 4 times on GalT and GalNAcT, respectively. It suggests that Mn^{2+} dependency of GalNAcT is higher than that of GalT. In comparison between PXS and PXR, PXS GalT was accelerated to 1.9 times although incase of PXR the Mn^{2+} enhancement was only 1.5 times fold. However, GalNAcT activation by Mn^{2+} was 4 times on both of strains. This result indicates that Mn^{2+} reception ability of PXR GalT was decreased by some mutations on Mn^{2+} binding site. On the other hand, the diversity of GalNAcT activity between PXS and PXR might not be the cause of mutations at site.

2.5.2. TLC analysis of labeled sugar incorporated glycolipid

Labeled galactose and GalNAc were incorporated into the glycosylceramides different from each other. Galactose incorporated glycosylceramides were detected as mono-, di-, tri-, tetra-, and >pentasaccharylceramide (Fig. 23, Galactose). However, this result embraces a contradiction. Generally, arthropod insects have characteristic glycosylceramide named arthro-series glycosylceramide (Wiegandt et al., 1992). Common structure of the glycolipid is GalNAcβ1-4GlcNAcβ1-3Manβ1-4Glcβ1Cer (Fig. 24A). However, the mono- to tetrasaccharylceramides incorporating galactose were detected by TLC analysis. If these oligosaccharylceramides are truly arthro-series glycosylceramide, then there should be a galactose residue on the down stream of 5^{th} residue. For that reason, galactose incorporated glycosylceramides may not be arthro-series; it is thought to be neogala-series rather than arthro-series. Neogala-series glycosylceramide is distributed over invertebrates such as platheliminthes (tapeworm etc.) and annelida (earthworm etc.) (Dennis et al., 1992; Hada et al., 2001). The most important characteristic point of the glycosylceramide is that first sugar residue is galactose, not glucose, and more galactose residues which are bound successively through β1-6 bond (Fig. 24B).

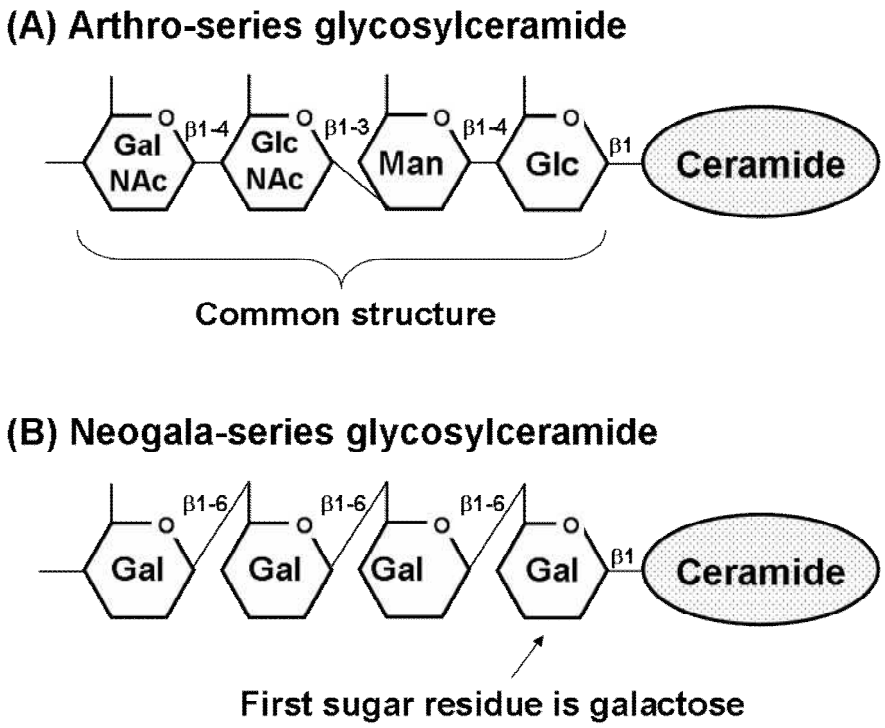

Fig. 24 Basic structure of invertebrate glycosylceramides. Invertebrate has many kinds of glycosylceramide. (A) Arthro-series glycosylceramide. This is a typical glycosylceramide found in arthropod including insect. Common structure of sugar side chain attached to arthro-series glycosylceramide is glucose, mannose, GlcNAc and GalNAc from reduced terminus. (B) Neogala-series glycosylceramide. It resides in platheliminthes (tapeworm etc.) and annelida (earthworm etc.). The most characteristic point of this glycosylceramide is that first sugar residue is galactose, and more galactose residues are bound through β1-6 bond.

As far as I know, it has not yet been reported that neogala-series glycosylceramide was also discovered in lepidopteran insect. But recently, it was made certain that there is the glycosylceramide in Zygomycetes, a kind of fungus (Aoki et al., 2004), indicating neogala-series glycosylceramide might be distributed widely among various organisms, therefore, the possibility that lepidopteron insect possessing glycosylceramide is considerable. Based on the hypothesis that galactose incorporated glycosylceramides must be neogala-series, I proposed the structure of each glycosylceramide (Fig. 25).

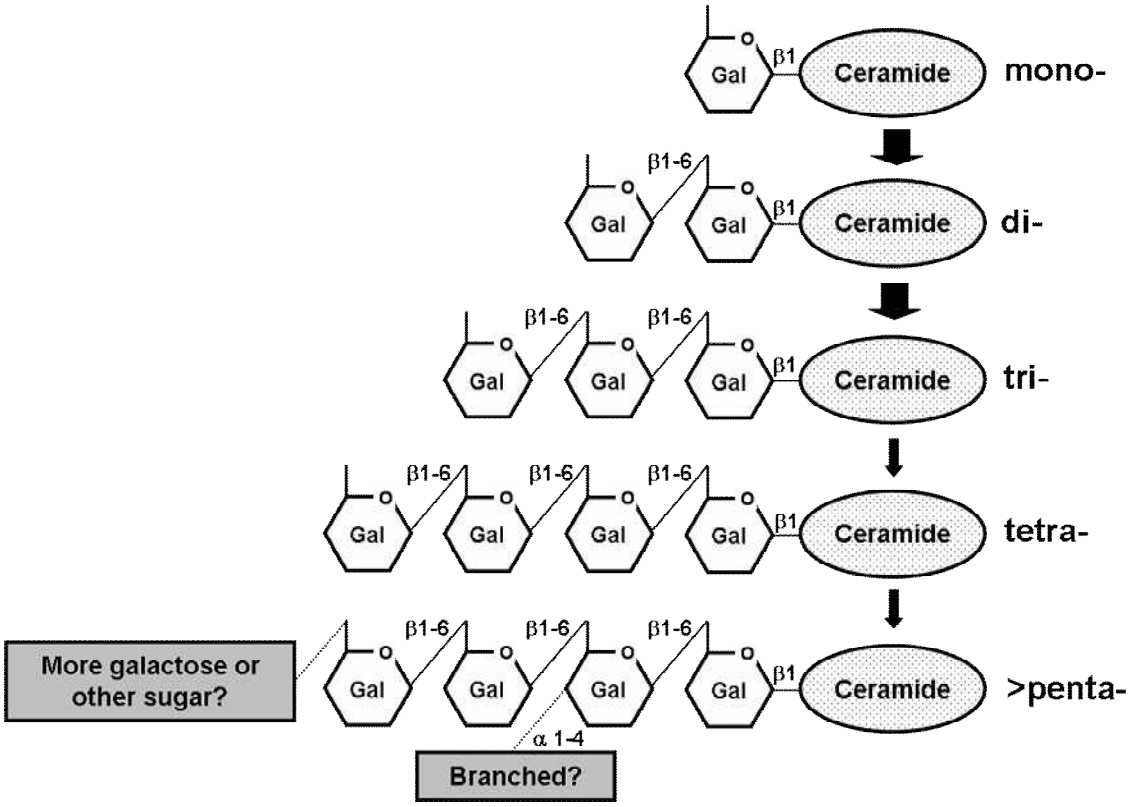

Fig. 25 Presumed structure of glycosylceramide incorporating galactose. Four galactose incorporated glycosylceramides were detected mainly on TLC analysis; mono, di, tri and tetrasaccharylceramide. All of these glycosylceramides may be categorized to neogala-series. Interestingly, the amount of mono- and disaccharylceramide were less than tri- and tetrasaccharylceramide. It suggests that galactosylation of mono- to disaccharylceramide and di- to trisaccharylceramide may be quick (thick arrow), but tri- to tetrasaccharylceramide and tetra- to >pentasaccharylceramide may be slow (thin arrow). >pentasaccharylceramide might be glycosylated more on 2nd or/and 4th galactose residue.

Sugar side chains attached to mono- to tetrasaccharylceramide may be composed of only β1-6 linked galactoses. Perhaps, >pentasaccharylceramide branches at 2nd galactose residue, or/and has more galactose or other sugars onto downstream of 4th residue. Interestingly, tri- and tetrasaccharylceramide were major components whereas mono- and disaccharylceramide were minor constituents. This result suggests that galactosylation from mono- to disaccharylceramide and di- to trisaccharylceramide may be quick in comparison with the additional reaction of tri- to tetrasaccharylceramide and the latter reactions. Indeed, the same tendency has been observed already neogala-series glycolipid synthesis *in vivo* (Aoki et al., 2004). It also supports strongly that galactose incorporated glycosylceramide must be neogala-series.

On the result of GalNAcT activity measurement using liquid scintillation counter, GalNAc incorporation into C/M solubilized fraction was very low (Fig. 21), and ignoring the effect of contaminated free UDP-GalNAc* in the sample was impossible. Therefore, it was unknown whether GalNAc was incorporated into the glycosylceramide or not. But I thought that GalNAc is incorporated actually into the glycolipid since GalNAc is an essential sugar constructed of the sugar side chain of arthro-series glycolipid described above. In fact, TLC analysis clarified that GalNAc also was taken into the glycosylceramide. GalNAc incorporated glycosylceramide was mainly tetrasaccharylceramide and may be categorized to arthro-series because 4th residue of arthro-series sugar side chain is just GalNAc (Fig. 23, GalNAc and Fig. 24A). >pentasaccharylceramide may branch at 4th GalNAc residue or/and has other sugar(s) on downstream of the residue through β1-4 bond (Fig. 26).

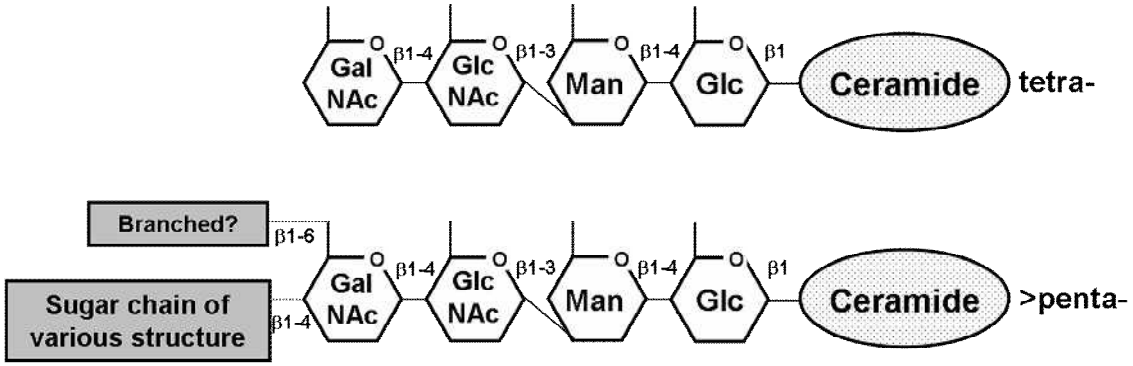

Fig. 26 Supposed structure of GalNAc incorporated glycosylceramide. Only two GalNAc incorporated glycosylceramides were detected on TLC analysis. These sugar side chains were exactly longer than trisaccharylceramide. Therefore, labeled GalNAc residue must be incorporated on 4th residue of the sugar side chain because GalNAc residue exists on the position in the common structure of arthro-series glycosylceramide. >pentasaccharylceramide might be added some sugars on GalNAc residue through ß1-4 or/and ß1-6 bond.

The most notable point of the TLC result is the amount of GalNAc incorporated tetrasaccharylceramide between PXS and PXR; it was remarkably more on PXS compared to PXR, showing clear direct evidence that GalNAcT activity of PXR for glycosylceramide synthesis is lower than PXS. Moreover, the decrease of GalNAcT activity must affect ≧pentasaccharylceramide synthesis because tetrasaccharylceramide is the precursor of ≧pentasaccharylceramide. In other words, loss of tetrasaccharylceramide may also raise reduction of ≧pentasaccharylceramide since sugar side chain synthesis is performed through step-by-step glycosylation from the reduced terminal. Indeed, Kumaraswami's report said that the neutral glycosylceramide amount of PXS was much higher than that of PXR especially on the ≧pentasaccharylceramide. The result of GalNAcT activity and TLC analysis described above supports to this Kumaraswami's report (Kumaraswami et al., 2001).

2.5.3. Hypothetical Cry1Ac resistant mechanism on PXR

Glycosyltransferase activity especially that of GalNAcT was higher on PXS in contrast to PXR, but the difference was 1.5-2 times at best (Fig. 21, Table 3). Apparently, it is not enough to prove to the >100,000 times Cry1Ac resistance of PXR, however, it can be satisfied. If total activity of some glycosyltransferase on PXR is extremely lower than PXS, it must be lethal mutation to PXR because glycosyltransferase is one of the essential enzymes for eukaryote. Actually, it was reported that total amount of the neutral glycolipid contained in PXS midgut is only two times higher than that of PXR (Kumaraswami et al., 2001). Therefore, I think that the glycolipid may perform the construction of hydrophobic microdomain of the BBM, i.e. raft region, rather than the receptor for Cry1Ac. On the **Chapter 1**, result of the oligomerization assay demonstrated that the raft region may function as interactive region to both monomeric and oligomeric Cry1A toxins (Fig. 12A and 13B, Insol.), and glycolipids are generally the major component of raft (Sato, 2001).

Based on these results described above and the previous repots, I hypothesized Cry1Ac resistance mechanism of PXR (Fig. 27).

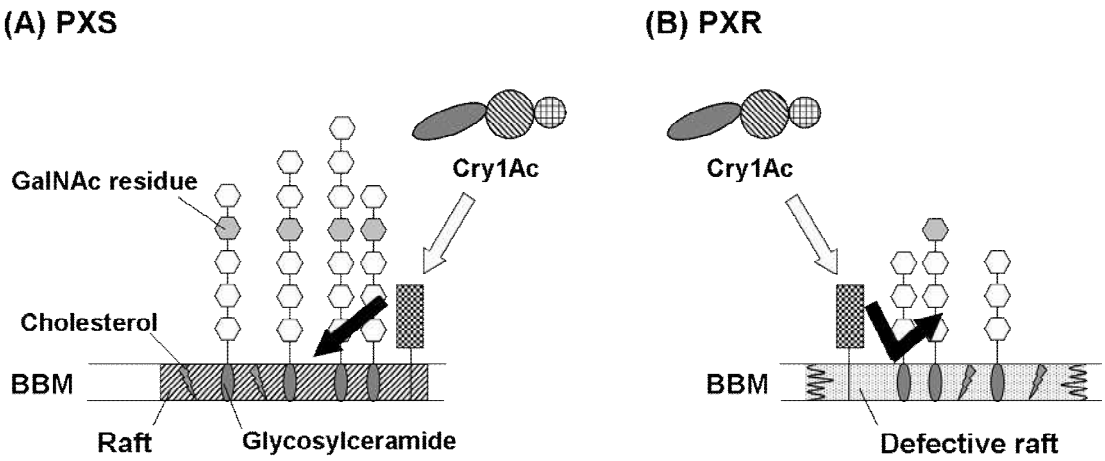

Fig. 27 Hypothesized Cry1Ac resistant mechanism on PXR. (A) PXS BBM. PXS BBM should contain sufficient glycosylceramides that have ≧5 sugar side chain. These glycosylceramides may support to construct of raft region on the BBM. Following Cry1Ac binding to specific receptor such as GPI anchored APN, Cry1Ac will interact with and insert into normal raft region, leading to form a pore on the BBM and the epithelial cell death. (B) PXR BBM. On the other hand, PXR may synthesize glycosylceramides that have relative short sugar side chain as the result of GalNAc transferase mutation. Consequently, defective raft region which invests no interactivity with Cry1Ac may constitute on the BBM. For that reason, Cry1Ac can not form a pore on the defective raft region whereas the receptor binding occurs ordinarily. White and black arrow represents the receptor binding and interaction with the membrane, respectively.

In PXS, metabolic pathway of glycosylceramide is normal, and the long-chain glycosylceramide is synthesized richly. As a result, ordinary raft region is constituted on the BBM and some GPI-anchored receptor such as APN distributed predominantly to raft region, binds with Cry1Ac. Consequently, Cry1Ac should insert into the region and form a pore, leading the insect death (Fig. 27A). On the other hand, glycosylceramide synthetic pathway of PXR may be disrupted by GalNAcT mutation, and the short-chain glycosylceramide may be synthesized mainly and transported toward the BBM. For that reason, defective raft should be constructed on the membrane and the region should not interact with Cry1Ac whereas the specific receptor binds with Cry1Ac (Fig. 27B). Thus, glycosylceramide component of the raft region that is hydrophobic microdomain of the BBM must be one of the crucial elements for Cry1Ac susceptibility and resistibility on *P. xylostella*.

3. Conclusion

I stated about the difference of insecticidal specificity between Cry1Aa and Cry1Ac against *B. mori* on the doctoral thesis. It was shown that the molecular conformation on *B. mori* BBM should widely differ between Cry1Aa and Cry1Ac. Moreover, I also mentioned Cry1Ac resistant mechanism of PXR. The most important result is that GalNAcT activity of PXR was lower than that of PXS and the tetrasaccharylceramide which is the precursor for ≧pentasaccharylceramide was slight on PXR compared to PXS.

I believe that Cry1A specificity and resistance mechanisms were solved partly, and then, these informations are useful to clarify Cry toxin`s mode of action. Finally, it will help to create the transgenic Cry toxin which has new insecticidal spectra and does not promote resistant insect.

4. Acknowledgement

I thank to Associate Professor Takuji Izumikawa and Assistant Professor Jun Goto (Radioisotope Center, Niigata University) for their invaluable technical support, and Dr. Takeshi Maruyama (Sumitomo Chemical Co., Ltd) and Dr. Kazuhisa Miyamoto (National Institute of Agriculture Science) for a donation of *P. xylostella*. Additionally, I am grateful to Professor Tsutomu Hoshino, Professor Toshiaki Mitsui, Professor Yoji Nakagawa and Associate Professor Keiichi Okazaki (Faculty of Agriculture, Niigata University) for the review of my doctoral thesis. And finally, I appreciate to Professor Hidetaka Hori, Associate professor Kimiko Itoh (Graduate School of Science and Technology, Niigata University) and Assistant Professor Tohru Hayakawa (Graduate School of Natural Science and Technology, Okayama University) for many beneficial advices and our laboratory colleagues for many kindnesses.

5. Reference

Adamczyk, J.Jr., Adams, L.C., Hardee, D.D., 2001. Field efficacy and seasonal expression profiles for terminal leaves of single and double *Bacillus thuringiensis* toxin cotton genotypes. J. Economic entomol. 94, 1589-1593.

Alcantara, E.P., Alzate, O., Lee, M.K., Curtiss, A., Dean, D.H., 2001. Role of α-helix seven of *Bacillus thuringiensis* Cry1Ab δ-endotoxin in membrane insertion, structural stability, and ion channel activity. Biochemistry 40, 2540-2547.

Aimanova, K.G., Zhuang, M., Gill, S.S., 2006. Expression of Cry1Ac cadherin receptors in insect midgut and cell lines. J. Inverteb. Pathol. 92, 178-187.

Angsuthanasombat, C., Uawithya, P., Leetachewa, S., Pornwiroon, W., Ounjai, P., Kerdcharoen, T., Katzenmeier, G., Panyim, S., 2004. *Bacillus thuringiensis* Cry4A and Cry4B mosquito-larvicidal proteins: homology-based 3D model and implications for toxin activity. J. Biochem. Mol. Biol. 37, 304-313.

Aoki, K., Uchiyama, R., Yamauchi, S., Katayama, T., Itonori, S., Sugita, M., Hada, N., Yamada-Hada, J., Takeda, T., Kumagai, H., Yamamoto, K., 2004. Newly discovered neutral glycosphingolipids in Aureobasidin A-resistant *Zygomycetes*. J. Biol. Chem. 279, 32028-32034.

Arnold, S., Curtiss, A., Dean, D.H., Alzate, O., 2001. The role of a proline-induced broken-helix motif in α-helix 2 of *Bacillus thuringiensis* δ-endotoxins. FEBS Lett. 490, 70-74.

Aronson A.I., Geng C., Wu L., 1999. Aggregation of *Bacillus thuringiensis* Cry1A toxins upon binding to target insect larval midgut vesicles. Appl. Environ. Microbiol. 65, 2503-2507.

Aronson, A.I., Shai, Y., 2001. Why *Bacillus thuringiensis* insecticidal toxins are so effective: unique features of their mode of action. FEMS Microbiol. Lett. 195, 1-8.

Avisar, D., Keller, M., Gazit, E., Prudovsky, E., Sneh, B., Zilberstein, A., 2004. The role of *Bacillus thuringiensis* Cry1C and Cry1E separate structural domains in the interaction with *Spodoptera littoralis* gut epithelial cells. J. Biol. Chem. 277, 15779-15786.

Banks, D.J., Jurat-Fuentes, J.L., Dean, D.H., Adang, M.J., 2001. *Bacillus thuringiensis* Cry1Ac and Cry1Fa δ-endotoxin binding to a novel 110 kDa aminopeptidase in *Heliothis virescens* is not *N*-acetylgalactosamine mediated. Insect Biochem. Mol. Biol. 31, 909-918.

Baxter, S.W., Zhao, J.Z., Gahan, L.J., Shelton, A.M., Tabashnik, B.E., Heckel, D.G., 2005. Novel genetic basis of field-evolved resistance to Bt toxins in *Plutella xylostella*. Insect Mol. Biol. 14, 327-334.

Boncheva, R., Dukiandjiev, S., Minkov, I., de Maagd, R.A., Naimov, S., 2006. Activity of *Bacillus thuringiensis* δ-endotoxins against codling moth (*Cydia pomonella* L.) larvae. J. Invert. Pathol. 92, 96-99.

Boonserm, P., Davis, P., Ellar, D.J., Li, J., 2005. Crystal structure of the mosquito-larvicidal toxin Cry4Ba and its biological implications. J. Mol. Biol. 348, 363-382.

Boonserm, T.K., Katzenmeier, P.G., Angsuthanasombat, C., 2005. Functional analysis of conserved aromatic residues in helix 7 critical for larvicidal activity of the *Bacillus thuringiensis* Cry4Ba toxin. In Abstract of the 4th International Conference on Biopesticides, Feb 13-18, Chiang Mai, Thailand. p103.

Bravo, A., Gómez, I., Conde, J., Muñoz-Garay, C., Sánchez, J., Miranda, R., Zhuang, M., Gill S.S., Soberón, M., 2004. Oligomerization triggers binding of a *Bacillus thuringiensis* Cry1Ab pore-forming toxin to aminopeptidase N receptor leading to insertion into membrane microdomains. Biochim. Biophys. Acta. 1667, 38-46.

Burkness, E.C., Hutchison, W.D., Bolin, P.C., Bartels, D.W., Warnock, D.F., Davis, D.W., 2001. Field Efficacy of sweet corn hybrids expressing a *Bacillus thuringiensis* toxin for management of *Ostrinia nubilalis* (Lepidoptera: Crambidae) and *Helicoverpa zea* (Lepidoptera: Noctuidae). J. Economic entomol. 94, 197-203.

Burton, S.L., Ellar, D.J., Li, J., Derbyshire, D.J., 1999. *N*-acetylgalactosamine on the putative insect receptor aminopeptidase N is recognized by a site on the domain III lectin-like fold of a *Bacillus thuringiensis* insecticidal toxin. J. Mol. Biol. 287, 1011-1022.

Carroll, J., Wolfersberger, M.G., Ellar, D.J., 1997. The *Bacillus thuringiensis* Cry1Ac toxin-induced permeability change in *Manduca sexta* midgut brush border membrane vesicles proceeds by more than one mechanism. J. Cell Science 110, 3099-3104.

Chandra, A., Ghosh, P., Mandaokar, A.D., Bera, A.K., Sharma, R.P., Das, S., Kumar, P.A., 1999. Amino acid substitution in α-helix 7 of Cry1Ac N-endotoxin of *Bacillus thuringiensis* leads to enhanced toxicity to *Helicoverpa armigera* Hubner. FEBS Lett. 458, 175-179.

Chen, J., Brown, M.R., Hua, G., Adang, M.J., 2005. Comparison of the localization of *Bacillus thuringiensis* Cry1A δ-endotoxins and their binding proteins in larval midgut of tobacco hornworm, *Manduca sexta*. Cell tissue res. 321, 123-129.

Cooper, M.A., Carroll, J., Travis, E.R., Williams, D.H., Ellar, D.J., 1998. *Bacillus thuringiensis* Cry1Ac toxin interaction with *Manduca sexta* aminopeptidase N in a model membrane environment. Biochem. J. 333, 677-683.

Crickmore, N., Zeigler, D.R., Feitelson, J., Schnepf, E., Van Rie, J., Lereclus, D., Baum, J., Dean, D.H., 1998. Revision of the nomenclature for the *Bacillus thuringiensis* pesticidal crystal proteins. Microbio. Mol. Biol. Rev. 62, 807-813.

de Maagd, R.A., Bakker, P.L., Masson, L., Adang, M.J., Sangadala, S., Stiekema, W., Bosch, D., 1999. Domain III of the *Bacillus thuringiensis* delta-endotoxin Cry1Ac is involved in binding to *Manduca sexta* brush border membranes and to its purified aminopeptidase N. Mol. Microbiol. 31, 463-471.

de Maagd, R.A., Bravo A., Crickmore, N., 2001. How *Bacillus thuringiensis* has evolved specific toxins to colonize the insect world. TRENDS in Genetics 17, 193-199.

de Maagd, R.A., Weemen-Hendriks, M., Stiekema, W., Bosch, D., 2000. *Bacillus thuringiensis* delta-endotoxin Cry1C domain III can function as a specificity determinant for *Spodoptera exigua* in different, but not all, Cry1-Cry1C hybrids. Appl. Environ. Microbiol. 66, 1559-1563.

Daniel, A., Dean, D.H., Adang, M.J., 2001. Analyses of the pore forming ability of *Bacillus thuringiensis* Cry1A mutant toxins using a light-scattering technique. Pesticide Biochem. Physiol. 70, 7-18.

Daniel, A., Sangadala, S., Dean, D.H., Adang, M.J., 2002. Denaturation of either *Manduca sexta* aminopeptidase N or *Bacillus thuringiensis* Cry1A toxins exposes binding epitopes hidden under nondenaturing conditions. Appl. Environ. Microbiol. 68, 2106–2112.

Dennis, R.D., Baumeister, S., Geyer, R., Peter-Katalinic, J., Hartmann, R., Egge, H., Geyer, E., Wiegandt, H., 1992. Glycosphingolipids in cestodes. Chemical structures of ceramide monosaccharide, disaccharide, trisaccharide and tetrasaccharide from metacestodes of the fox tapeworm, *Taenia crassiceps* (*Cestoda: Cyclophyllidea*). Eur. J. Biochem. 207, 1053-1062.

Denolf, P., Hendrickx, K., Van Damme, J., Jansens, S., Peferoen, M., 1997. Cloning and characterization of *Manduca sexta* and *Plutella xylostella* midgut aminopeptidase N enzymes related to *Bacillus thuringiensis* toxin-binding proteins. Eur. J. Biochem. 248, 748-761.

Dorsch, J.A., Candas, M., Griko, N.B., Maaty, W.S.A., Midboe, E.G., Vadlamudi, R.K., Bulla, L.A.Jr., 2002. Cry1A toxins of *Bacillus thuringiensis* bind specifically to a region adjacent to the membrane-proximal extracellular domain of BT-R_1 in *Manduca sexta*: involvement of a cadherin in the entomopathogenicity of *Bacillus thuringiensis*. Insect biochem. Mol. Biol. 32, 1025-1036.

Duché, D., Parkere, M.W., González-Mañas, J.M., Pattus, F., Baty, D., 1994. Uncoupled steps of the colicin A pore formation demonstrated by disulfide bond engineering. J. Biol. Chem. 269, 6332-6339.

Fernández, L.E., Pérez, C., Segovia, L., Rodrĺguez, M.H., Gill, S.S., Bravo, A., Soberón, M., 2005. Cry11Aa toxin from Bacillus thuringiensis binds its receptor in *Aedes aegypti* mosquito larvae through loop α-8 of domain II. FEBS Lett. 579, 3508-3514.

Ferre, J., Real, M.D., Rie, J.V., Jansens, S., Peferoen, M., 1991. Resistance to the *Bacillus thuringiensis* bioinsecticide in a Field Population of *Plutella xylostella*. Proc. Natl. Acad. Sci. USA. 88, 5119-5123.

Flannagan, R.D., Yu, C.G., Mathis, J.P., Meyer, T.E., Shi, X., Siqueira, H.A., Siegfried, B.D., 2005. Identification, cloning and expression of a Cry1Ab cadherin receptor from European corn borer, *Ostrinia nubilalis* (Hubner) (Lepidoptera: Crambidae). Insect biochem. Mol. Biol. 35, 33-40.

Gahan, L.J., Gould, F., Heckel, D.G., 2001. Identification of a gene associated with Bt resistance in *Heliothis virescens*. Science 293, 857-860.

Garczynski, S.F., Adang, M.J., 1995. *Bacillus thuringiensis* Cry1A(c) δ-endotoxin binding aminopeptidase in the *Manduca sexta* midgut has a glycosyl-phosphatidylinositol anchor. Insect Biochem. Mol. Biol. 25, 409-415.

Garner, K.J., Hiremath, S., Lehtoma, K., Valaitis, A.P., 1999. Cloning and complete sequence characterization of two gypsy moth aminopeptidase-N cDNAs, including the receptor for *Bacillus thuringiensis* Cry1Ac toxin. Insect Biochem. Mol. Biol. 29, 527-535.

Gazit, E., Bach, D., Kerr, I.D., Sansom, M.S.P., Chejanovsky, N., Shai, Y., 1994. The α-5 segment of *Bacillus thuringiensis* δ-endotoxin: in vitro activity, ion channel formation and molecular modeling. Biochem. J. 304, 895-902.

Gazit, E., Rocca, P.L., Sansom, M.S.P., Shai, Y., 1998. The structure and organization within the membrane of the helices composing the pore-forming domain of *Bacillus thuringiensis* δ-endotoxin are consistent with an “umbrella-like” structure of the pore. Proc. Natl. Acad. Sci. USA. 95, 12289-12294.

Gazit, E., Shai, Y., 1995. The assembly and organization of the α5 and α7 helices from the pore-forming domain of *Bacillus thuringiensis* δ-endotoxin. J. Biol. Chem. 277, 2571-2578.

Ge, A.Z., Rivers, D., Milne, R., Dean, D.H., 1991. Functional domains of *Bacillus thuringiensis* insecticidal crystal proteins. J. Biol. Chem. 266, 17954-17958.

Gerber, D., Shai, Y., 2000. Insertion and organization within membranes of the δ-endotoxin pore-forming domain, helix 4-loop-helix 5, and inhibition of its activity by a mutant helix 4 peptide. J. Biol. Chem. 275, 23602-23607.

Gill, S.S., Cowles, E.A., Francis, V., 1995. Identification, isolation, and cloning of a *Bacillus thuringiensis* CryIAc toxin-binding protein from the midgut of the lepidopteran insect *Heliothis virescens*. J. Biol. Chem. 270, 27277-27282.

Gómez, I., Miranda-Rios, J., Rudinõ-Piñera, E., Oltean, D.I., Gill, S.S., Bravo, A., Soberón, M., 2002a. Hydropathic complementarity determines interaction of epitope ^{869}HITDTNNK^{876} in *Manduca sexta* Bt-R_1 receptor with loop 2 of domain II of *Bacillus thuringiensis* Cry1A toxins. J. Biol. Chem. 277, 30137-30143.

Gómez, I., Oltean, D.I., Gill, S.S., Bravo, A., Soberón, M., 2001. Mapping the epitope in cadherin-like receptors involved in *Bacillus thuringiensis* Cry1A toxin interaction using phage display. J. Biol. Chem. 276, 28906-28912.

Gómez, I., Sánchez, J., Miranda, R., Bravo, A., Soberón, M., 2002b. Cadherin-like receptor binding facilitates proteolytic cleavage of helix α-1 in domain I and oligomer pre-pore formation of *Bacillus thuringiensis* Cry1Ab toxin. FEBS Lett. 513, 242-246.

González-Cabrera, J., Escriche, B., Tabashnik, B.F., Ferré, J., 2003. Binding of *Bacillus thuringiensis* toxins in resistant and susceptible strains of pink bollworm (*Pectinophora gossypiella*). Insect biochem. Mol. Biol. 33, 929-935.

González-Cabrera, J., Herrero, S., Sayyed, A.H., Escriche, B., Liu, Y.B., Meyer, S.K., Wright, D.J., Tabashnik, B.E., Ferre, J., 2001. Variation in susceptibility to *Bacillus thuringiensis* toxins among unselected strains of *Plutella xylostella*. Appl. Environ. Microbiol. 67, 4610-4613.

Greenfield, L., Bjorn, M.J., Horn, G., Fong, D., Buck, G.A., Collier, R.J., Kaplan, D.A., 1983. Nucleotide sequence of the structural gene for diphtheria toxin carried by corynebacteriophage β. Proc. Natl. Acad. Sci. USA. 80, 6853-6857.

Griffitts, J.S., Aroian, R.V., 2005. Many roads to resistance: how invertebrates adapt to Bt toxins. BioEssays 27, 614-624.

Griffitts, J.S., Haslam, S.M., Yang, T., Garczynski, S.F., Mulloy, B., Morris, H., Cremer, P.S., Dell, A., Adang, M.J., Aroian, R.V., 2005. Glycolipids as receptors for *Bacillus thuringiensis* crystal toxin. Science 307, 922-925.

Griffitts, J.S., Huffman, D.L., Whitacre, J.L., Barrows, B.D., Marroquin, L.D., Müller, R., Brown, J.R., Hennet, T., Esko, J.D., Aroian, R.V., 2003. Resistance to a bacterial toxin is mediated by removal of a conserved glycosylation pathway required for toxin-host interactions. J. Biol. Chem. 278, 45594-45602.

Griffitts, J.S., Whitacre, J.L., Stevens, D.E., Aroian, R.V., 2001. Bt toxin resistance from loss of a putative carbohydrate-modifying enzyme. Science 293, 860-864.

Grochulski, P., Masson, L., Borisova, S., Pusztai-Carey, M., Schwartz, J.L., Brousseau, R., Cygler, M., 1995. *Bacillus thuringiensis* CryIA(a) insecticidal toxin: Crystal structure and channel formation. J. Mol. Biol. 254, 447-464.

Güereca, L., Bravo, A., 1999. The oligomeric state of *Bacillus thuringiensis* Cry toxins in solution. Biochim. Biophys. Acta. 1429, 342-350.

Hada, N., Sato, K., Sakushima, J., Goda, Y., Sugita, M., Takeda, T., 2001. Synthetic studies on glycosphingolipids from protostomia phyla: Synthesis of amphoteric glycolipid analogues containing a phosphocholine residue from the earthworm *Pheretima hilgendorfi*. Chem. Pharm. Bull. 49, 1464-1467.

Hayakawa, T., Shitomi, Y., Miyamoto, K., Hori, H., 2004. *Bacillus thuringiensis* Cry1Ac was trapped on the peritrophic membrane of *Bombyx mori*, but pretreatment with GalNAc inhibited the trapping. FEBS Lett. 576 331-335.

He, K., Wang, Z., Bai, S., Zheng, L., Wang, Y., Cui, H., 2006. Efficacy of transgenic Bt cotton for resistance to the Asian corn borer (Lepidoptera: Crambidae). Crop Protection 25, 167-173.

Hernández, C.S., Ferré, J., 2005. Common receptor for *Bacillus thuringiensis* toxins Cry1Ac, Cry1Fa, and Cry1Ja in *Helicoverpa armigera*, *Helicoverpa zea*, and *Spodoptera exigua*. Appl. Environ. Microbiol. 71, 5627-5629.

Herrero, S., Gechev, T., Bakker1, P.L., Moar, W.J., de Maagd, R.A., 2005. *Bacillus thuringiensis* Cry1Ca-resistant *Spodoptera exigua* lacks expression of one of four aminopeptidase N genes. BMC Genomics 6, 96-105.

Höfte,H., Whiteley, H.R., 1989. Insecticidal crystal protein of *Bacillus thuringiensis*. Microbiol. Rev. 53, 242-255.

Hossain, D.M., Shitomi,Y., Moriyama, K., Higuchi, M., Hayakawa, T., Mitsui, T., Sato, R., Hori1., H, 2004. Characterization of a novel plasma membrane protein, expressed in the midgut epithelia of *Bombyx mori*, that binds to Cry1A toxins. Appl. Environ. Microbiol. 70, 4604-4612.

Hua, G., Masson, L., Jurat-Fuentes, J.L., Schwab, G., Adang., M.J., 2001. Binding analyses of *Bacillus thuringiensis* Cry δ-endotoxins using brush border membrane vesicles of *Ostrinia nubilalis*. Appl. Environ. Microbiol. 67, 872-879.

Ihara, H., Uemura, T., Masuhara, M., Ikawa, S., Sugimoto, K., Wadano, A., Himeno, M., 1998. Purification and partial amino acid sequences of the binding protein from *Bombyx mori* for CryIAa d-endotoxin of *Bacillus thuringiensis*. Comp. Biochem. Physiol. B. 120, 197-204.

International Service for the Acquisition of Agri-biotech Applications, 2005. Global Status of Commercialized Biotech/GM Crops: 2005.

Ivanov, D.B., Philippova, M.P., Tkachuk, V.A., 2001. Structure and functions of classical cadherins. Biochemistry (Moscow) 66, 1450-1464.

Jenkins, J.L., Dean, D.H., 2001. Binding specificity of *Bacillus thuringiensis* Cry1Aa for purified, native *Bombyx mori* aminopeptidase N and cadherin-like receptors. BMC Biochemistry 2, 12.

Johnson, P.E., Manish, D.J., Tomme, P., Kilburn, D.G., McIntosh, L.P., 1996. Structure of the N-terminal cellulose-binding domain of *Cellulomonas fimi* CenC determined by nuclear magnetic resonance spectroscopy. Biochemistry 35, 14381-14394.

Jurat-Fuentes, J.L., Adang, M.J., 2001. Importance of Cry1 δ-endotoxin domain II loops for binding specificity in *Heliothis virescens* (L.). Appl. Environ. Microbiol. 67, 323-329.

Jurat-Fuentes, J.L., Gould, F.L., Adang1, M.J., 2002. Altered glycosylation of 63- and 68-kilodalton microvillar proteins in *Heliothis virescens* correlates with reduced Cry1 toxin binding, decreased pore formation, and increased resistance to *Bacillus thuringiensis* Cry1 toxins. Appl. Environ. Microbiol. 68, 5711–5717.

Karlova, R., Weemen-Hendriks, M., Naimova, S., Ceronc, J., Dukiandjiev, S., de Maag, R.A., 2005. *Bacillus thuringiensis* δ-endotoxin Cry1Ac domain III enhances activity against *Heliothis virescens* in some, but not all Cry1-Cry1Ac hybrids. J. Invert. Pathol. 88, 169-172.

Kanintronkul, Y., Sramala, I., Katzenmeier, G., Panyim, S., Angsuthanasombat, C., 2003. Specific mutations within the α4-α5 loop of the *Bacillus thuringiensis* Cry4B toxin reveal a crucial role of Asn-166 and Tyr-170. Mol. Biotechnol. 24, 11-19.

Kato, T., Higuchi, M., Endo, R., Maruyama, T., Haginoya, K., Shitomi, Y., Hayakawa, T., Mitsui, T., Sato, R., Hori, H., 2006. *Bacillus thuringiensis* Cry1Ab, but not Cry1Aa or Cry1Ac, disrupts liposomes. Pesticide Biochem. Physiol. 84, 1-9.

Knight, P.J.K., Crickmore, N., Ellar, D.J., 1994. The receptor for *Bacillus thuringiensis* CryIA(c) d-endotoxin in the brush border membrane of the lepidopteran *Manduca sexta* is aminopeptidase N. Mol. Microbiol. 11, 429-436.

Knight, P.J.K., Knowles, B.H., Ellar, D.J., 1995. Molecular cloning of an insect aminopeptidase N that serves as a receptor for *Bacillus thuringiensis* CryIA(c) toxin. J. Biol. Chem. 270, 17765-17770.

Knowles, B.H., 1994. Mechanism of action of *Bacillus thuringiensis* insecticidal Deltaendotoxins. Adv. Insect Physiol. 24, 275-308.

Knowles, B.H., Ellar, D.J., 1987. Colloid-osmotic lysis is a general feature of the mechanism of action of *Bacillus thuringiensis* δ-endotoxin with different insect specificity. Biochim. Biophys. Acta. 924, 509-518.

Kumar, H., Kumar, V., 2004. Tomato expressing Cry1A(b) insecticidal protein from *Bacillus thuringiensis* protected against tomato fruit borer, *Helicoverpa armigera* (Hübner) (Lepidoptera: Noctuidae) damage in the laboratory, greenhouse and field. Crop Protection 23, 135-139.

Kumar, N.S., Venkateswerlu, G., 1998. Intracellular proteases in sporulated *Bacillus thuringiensis* subsp. *kurstaki* and their role in protoxin activation. FEMS Microbiol. Lett. 166, 377-382.

Kumaraswami, N.S., Maruyam, T., Kurabe, S., Kishimoto, T., Mitsui, T., Hori, H., 2001. Lipids of brush border membrane vesicles BBMV from *Plutella xylostella* resistant and susceptible to Cry1Ac δ-endotoxin of *Bacillus thuringiensis*. Comp. Biochem. Physiol. B. 129, 173-183.

Laemmli, U.K., 1970. Cleavage of structural proteins during the assembly of the head of bacteriophage T4. Nature. 227, 680-685.

Lee, M.K., Rajamohan, F., Jenkins, J.L., Curtiss, A.S., Dean, D.H., 2000. Role of two arginine residues in domain II, loop 2 of Cry1Ab and Cry1Ac *Bacillus thuringiensis* δ-endotoxin in toxicity and binding to *Manduca sexta* and *Lymantria dispar* aminopeptidase N. Mol. Microbiol. 38, 289-298.

Li, J., Carroll, J., Ellar, D.J., 1991. Crystal structure of insecticidal delta–endotoxin from *Bacillus thuringiensis* at 2.5 Å resolution. Nature. 353, 815-821.

Lu, H., Rajamohan, F., Dean, D.H., 1994. Identification of amino acid residues of *Bacillus thuringiensis* δ-endotoxin CryIA(a) associated with membrane binding and toxicity to *Bombyx mori*. J. Bacteriol. 176, 5554-5559.

Luo, K., Sangadala, S., Masson, L., Mazza, A., Brousseau R., Adang, M.J., 1997. The *Heliothis virescens* 170 kDa aminopeptidase functions as "Receptor A" by mediating specific *Bacillus thuringiensis* Cry1A δ-endotoxin binding and pore formation. Insect biochem. Mol. Biol. 27, 735-743.

Luo, S., Wang, G., Liang, G., Wu, K.M., Bai, L., Ren, X., Guo Y., 2006. Binding of three Cry1A toxins in resistant and susceptible strains of cotton bollworm (*Helicoverpa armigera*). Pesticide Biochem. Physiol. 85, 104-109.

McNall, R.J., Adang, M.J., 2003. Identification of novel *Bacillus thuringiensis* Cry1Ac binding proteins in *Manduca sexta* midgut through proteomic analysis. Insect Biochem. Mol. Biol. 33, 999-1010.

Martinez-Ramirez, A.C., Gonzalez-Nebauer, S., Esriche, B., Real, M.D., 1994. Ligand blot identification of a *Manduca sexta* midgut binding protein specific to three *Bacillus thuringiensis* Cry1A-type ICPs. Biochem. Biophys. Res. Commun. 201, 782-787.

Maruyama, T., Hama, H., Asano, S., 1999. Establishment and maintenance of high resistance to *Bacillus thuringiensis* formulation in diamondback moth, *Plutella xylostella* (Lepidoptre: Yponomeutidae). Jpn. J. Appl. Entomol. Zool. 43, 7-12. (Japanese article with English abstract).

Masson, L., Lu, Y., Mazza, A., Brousseau, R., Adang, M.J., 1995. The CryIA(c) receptor purified from *Manduca sexta* displays multiple specificities. J. Biol. Chem. 270, 20309-20315.

Masson, L., Tabashnik, B.E., Liu, Y.B., Brousseau, R., Schwartz, J.L., 1999. Helix 4 of the *Bacillus thuringiensis* Cry1Aa toxin lines the lumen of the ion channel. J. Biol. Chem. 274, 31996-32000.

Milne, R., Kaplan, H., 1993. Purification and characterization of a trypsin-like digestive enzyme from spruce budworm (*Chroristoneura fumiferana*) responsible for the activation of δ-endotoxin from *Bacillus thuringiensis*. Insect biochem. Mol. Biol. 23, 663-673.

Miranda, R., Zamudio, F.Z., Bravo, A., 2001. Processing of Cry1Ab δ-endotoxin from *Bacillus thuringiensis* by *Manduca sexta* and *Spodoptera frugiperda* midgut proteases: role in protoxin activation and toxin inactivation. Insect biochem. Mol. Biol. 31, 1155-1163.

Murata, K., Mitsuoka, K., Hirai, T., Walz, T., Agre, P., Heymann, J.B., Engel, A., Fujiyoshi, Y., 2000. Structural determinants of water permeation through aquaporin-1. Nature 407, 599-605.

Murzin, A.G., Bateman, A., 1997. Distant homology recognition using structural classification of proteins. Proteins Suppl. 1, 92-104.

Nagamatsu, Y., Koike, T., Sasaki, K., Yoshimoto, A., Furukawa, Y., 1999. The cadherin-like protein is essential to specificity determination and cytotoxic action of the *Bacillus thuringiensis* insecticidal CryIAa toxin. FEBS Lett. 460, 385-390.

Nagamatsu, Y., Toda, S., Koike, T., Miyoshi, Y., Shigematsu, S., Kogure, M., 1998a. Cloning, sequencing, and expression of the *Bombyx mori* receptor for *Bacillus thuringiensis* insecticidal CryIA(a) toxin. Biosci. Biotechnol. Biochem. 62, 727-734.

Nagamatsu, Y., Toda, S., Yamaguchi, F., Ogo, M., Kogure, M., Nakamura, M., Shibata, Y., Katsumoto, T., 1998b. Identification of *Bombyx mori* midgut receptor for *Bacillus thuringiensis* insecticidal CryIA(a) toxin. Biosci. Biotechnol. Biochem. 62, 718-726.

Nakanishi, K., Yaoi, K., Nagino, Y., Hara, H., Kitami, M., Atsumi, S., Miura, N., Sato, R., 2002. Aminopeptidase N isoforms from the midgut of *Bombyx mori* and *Plutella xylostella* - their classification and the factors that determine their binding specificity to *Bacillus thuringiensis* Cry1A toxin. FEBS Lett. 519, 215-220.

Ogiwara, K., Indrasith, L.S., Asano, S., Hori, H., 1992. Processing of δ-endotoxin from *Bacillus thuringiensis* subsp. kurstaki HD-1 and HD-73 by gut juice of various insect larvae. J. Invertebr. Pathol. 60, 121-126.

Oltean, D.I., Pullikuth, A.K., Lee, H.-K., Gill, S., 1999. Partial purification and characterization of *Bacillus thuringiensis* Cry1A toxin receptor A from *Heliothis virescens* and cloning of the corresponding cDNA. Appl. Environ. Microbiol. 65, 4760-4766.

Oppert B., Kramer K.J., Johnson D.E., Macintosh S.C., Mcgaughey, W.H., 1994. Altered protoxin activation by midgut enzymes from a *Bacillus thuringiensis* resistant strain of *Plodia interpunctella*. Biochem. Biophysic. Res. Commu. 198, 940-947.

Puntheranurak, T., Uawithya, P., Potvin, L., Angsuthanasombat, C., Schwartz, J.-L., 2004. Ion channels formed in planar lipid bilayers by the dipteran-specific Cry4B *Bacillus thuringiensis* toxin and its α1-α5 fragment. Mol. Membrane biol. 21, 67-74.

Rajamohan, F., Hussain, S.-R.A., Cotrill, J.A., Gould, F., Dean, D.H., 1996. Mutations at domain II, loop 3, of *Bacillus thuringiensis* CryIAa and CryIAb δ-endotoxins suggest loop 3 is involved in initial binding to lepidopteran midguts. J. Biol. Chem. 271, 25220-25226.

Rausell, C., Muñoz-Garay, C., Miranda-CassoLuengo, R., Gómez, I., Rudiño-Piñera, E., Soberón, M., Bravo, A., 2004. Tryptophan spectroscopy studies and black lipid bilayer analysis indicate that the oligomeric structure of Cry1Ab toxin from *Bacillus thuringiensis* is the membrane-insertion intermediate. Biochemistry 43, 166-174.

Rausell, C., Pardo-López, L., Sánchez, J., Muñoz-Garay, C., Morera, C., Soberón, M., Bravo, A., 2004. Unfolding events in the water-soluble monomeric Cry1Ab toxin during transition to oligomeric pre-pore and membrane-inserted pore channel. J. Biol. Chem. 279, 55168-55175.

Sangadala, S., Azadi, P., Carlson, R., Adang, M.J., 2001. Carbohydrate analyses of *Manduca sexta* aminopeptidase N, co-purifying neutral lipids and their functional interactions with *Bacillus thuringiensis* Cry1Ac toxin. Insect Biochem. Mol. Biol. 32, 97-107.

Sangadala, S., Walters, F.S., English, L.H., Adang, M.J., 1994. A mixture of *Manduca Sexta* aminopeptidase and phosphatase enhances *Bacillus thuringiensis* insecticidal CryIA(c) toxin binding and $^{86}Rb^{(+)}$-$K^{(+)}$ efflux in vitro. J. Biol. Chem. 269, 10088-10092.

Sato, T., 2001. The physicochemical study on the formation of glycolipid domain. Trends. Glycosci. Glycotechnol. 13, 231-238.

Sayyed, A.H, Haward, R., Herrero, S., Ferré, J., Wrigh, D.J., 2000. Genetic and biochemical approach for characterization of resistance to *Bacillus thuringiensis* toxin Cry1Ac in a field population of the diamondback moth, *Plutella xylostella*. Appl. Environ. Microbiol. 66, 1509-1516.

Schnepf, E., Crickmore, N., Van Rie, J., Lereclus, D., Baum, J., Feitelson, J., Zeigler, D.R., Dean, D.H., 1998. *Bacillus thuringiensis* and its pesticidal crystal protein. Microbiol. Mol. Biol. Rev. 62, 775-806.

Schnepf, H.E., Tomczak, K., Ortega, J.P., Whiteley, H.R., 1990. Specificity-determining regions of a Lepidopteran-specific insecticidal protein produced by *Bacillus thuringiensis*. J. Biol. Chem. 265, 20923-20930.

Schwartz, J.-L., Lu, Y.J., Soehnlein, P., Brousseau, R., Masson, L., Laprade, R., Adang, M.J., 1997. Restriction of intermolecular movements within the Cry1Aa toxin molecule of *Bacillus thuringiensis* through disulfide bond engineering. FEBS Lett. 410, 397-402.

Shitomi, Y., Hayakawa, T., Hossain, D.M., Higuchi, M., Miyamoto, K., Nakanishi, K., Sato, R., Hori, H., 2006. A novel 96-kDa aminopeptidase localized on epithelial cell membrane of *Bombyx mori* midgut, which binds to Cry1Ac toxin of *Bacillus thuringiensis*. J. Biochem. 139, 223-233.

Simpson, R.M., Newcomb, R.D., 2000. Binding of *Bacillus thuringiensis* δ-endotoxins Cry1Ac and Cry1Ba to a 120-kDa aminopeptidase-N of *Epiphyas postvittana* purified from both brush border membrane vesicles and baculovirus-infected Sf9 cells Insect Biochem. Mol. Biol. 30, 1069-1078.

Siqueira, H.A.A., González-Cabrera, J., Ferré, J., Flannagan, R., Siegfried, B.D., 2006. Analyses of Cry1Ab Binding in Resistant and Susceptible Strains of the European Corn Borer, *Ostrinia nubilalis* (Hübner) (Lepidoptera: Crambidae) Appl. Environ. Microbiol. 72, 5318-5324.

Suzuki, N., Hori, H., Ogiwara, K., Asano, S., Sato, R., Ohba, M., Iwahana, H., 1992. Insecticidal spectrum of a novel *Bacillus thuringiensis* serovar *japonensis*. Biological Control. 2, 138-142.

Tabashnik, B.E., 1994a. Evolution of resistance to *Bacillus thuringiensis*. Annu. Rev. Entomol. 39, 7-49.

Tabashnik, B.E., Finson, N., Groeters, F.R., Moar, W. J., Johnson, M.W., Luo, K., Adang M.J., 1994b. Reversal of resistance to *Bacillus thuringiensis* in *Plutella xylostella*. Proc. Natl. Acad. Sci. USA. 91, 4120-4124.

Tigue, N.J., Jacoby, J., Ellar, D.J., 2001. The α-helix 4 residue, ASN135, is involved in the oligomerization of Cry1Ac1 and Cry1Ab5 *Bacillus thuringiensis* toxins. Appl. Environ. Microbiol. 67, 5715-5720.

Tran, L.B., Vachon, V., Schwartz, J.L., Laprade, R., 2001. Differential effects of pH on the pore-forming properties of *Bacillus thuringiensis* insecticidal crystal toxins. Appl. Environ. Microbiol. 67, 4488-4494.

Vadlamudi, R.K., Weber, E., Ji, I., Ji, T.H., Bulla, L.A.Jr., 1995. Cloning and expression of a receptor for an insecticidal toxin of *Bacillus thuringiensis*. J. Biol. Chem. 270, 5490-5494.

Vachon, V., Préfontaine, G., Coux, F., Rang, C., Marceau, L., Masson, L., Brousseau, R., Frutos, R., Schwartz, J.L., Laprade, R., 2002. Role of helix 3 in pore formation by the *Bacillus thuringiensis* insecticidal toxin Cry1Aa. Biochemistry 41, 6178-6184.

Valaitis, A.P., Lee, M.K., Rajamohan, F., Dean, D.H., 1995. Brush border membrane aminopeptidase-N in the midgut of the gypsy moth serves as the receptor for the CryIA(c) δ-endotoxin of *Bacillus thuringiensis*. Insect Biochem. Mol. Biol. 25, 1143-1151.

Van Rie, J., McGaughey, W.H., Johnson, D.E., Barnett, D.E., Van Mellaert, H., 1990. Mechanism of insect resistance to the microbial insecticide *Bacillus thuringiensis*. Science 247, 72-74.

Walters, F.S., Slatin, S.L., Kulesza, C.A., English, L.H., 1993. Ion channel activity of N-terminal fragments from CryIA(c) δ-endotoxin. Biochem. Biophys. Res. Commun. 196, 921-926.

Wan, P., Wu, K., Huang, M., Wu, J., 2004. Seasonal pattern of infestation by pink bollworm *Pectinophora gossypiella* (Saunders) in field plots of Bt transgenic cotton in the Yangtze River valley of China. Crop Protection 23, 463-467.

Wiegandt, H., 1992. Insect glycolipids. Biochim. Biophys. Acta. 1123, 117-126.

Wirth, M.C., Delécluse, A., Federici, B.A., Walton, W.E., 1998. Variable cross-resistance to Cry11B from *Bacillus thuringiensis* subsp. *jegathesan* in *Culex quinquefasciatus* (Diptera: Culicidae) resistant to single or multiple toxins of *Bacillus thuringiensis* subsp. *israelensis*. Appl. Environ. Microbiol. 64, 4174-4179.

Wolfersberger, M., Luethy, P., Maurer, A., Parenti, P., Sacchi, F.V., Gioedana, B., Hanozet, G.M., 1987. Preparation and partial characterization of amino acid transporting brush border membrane vesicles from the larval midgut of the cabbage butterfly (*Pieris Brassicae*). Comp. Biochem. Physiol. A. 86, 301-308.

Xie, R., Zhuang, M., Ross, L.S., Gómez, I., Oltean, D.I., Bravo, A., Soberón, M., Gill, S.S., 2005. Single amino acid mutations in the cadherin receptor from *Heliothis virescens* affect its toxin binding ability to Cry1A toxins. J. Biol. Chem. 280, 8416-8425.

Yaoi, K., Nakanishi, K., Kadotani, T., Imamura, M., Koizumi, N., Iwahana, H., Sato, R., 1999a. *Bacillus thuringiensis* Cry1Aa toxin-binding region of *Bombyx mori* aminopeptidase N. FEBS Lett. 463, 221-224.

Yaoi, K., Nakanishi, K., Kadotani, T., Imamura, M., Koizumi, N., Iwahana, H., Sato, R., 1999b. cDNA cloning and expression of *Bacillus thuringiensis* Cry1Aa toxin binding 120 kDa aminopeptidase N from *Bombyx mori*. Biochim. Biophys. Acta. 1444, 131-137.

Zhao, J.Z., Cao, J., Li, Y., Collins, H.L., Roush, R.T., Earle, E.D., Shelton, A.M., 2003. Transgenic plants expressing two *Bacillus thuringiensis* toxins delay insect resistance evolution. Nature Biotechnol. 21, 1493-1497.

Zhao, J.Z., Collins, H.L., Tang, J.D., Cao, J., Earle, E.D., Roush, R.T., Herrero, S., Escriche, B., Ferré, J., Shelton, A.M., 2000. Development and characterization of diamondback moth resistance to transgenic broccoli expressing high levels of Cry1C. Appl. Environ. Microbiol. 66, 3784-3789.

Zhuang, M., Oltean, D.I., Gómez, I., Pullikuth, A.K., Soberón, M., Bravo, A., Gill, S.S., 2002. *Heliothis virescens* and *Manduca sexta* lipid rafts are involved in Cry1A toxin binding to the midgut epithelium and subsequent pore formation. J. Biol. Chem. 277, 13863-13872.